Electronic Supplementary Material (ESI) for Green Chemistry.

Supporting Information

Beyond biodegradation: upcycling of polylactic acid plastic wastes into amino acids via cascade catalysis under mild conditions

Yingxin Ma[a,1], Xuyun Guo[e,1], Mengmeng Du[a], Sailei Kang[a], Weiliang Dong[d], Valeria Nicolosi[e], Zhongli Cui[c], Yu Zhang*[b], and Bocheng Qiu*[a].

[a] Department of Chemistry, College of Sciences, Nanjing Agricultural University, Nanjing 210095, China. E-mail: bochengqiu@njau.edu.cn
[b] College of Energy and Power Engineering, Nanjing Institute of Technology, Nanjing 211167, China. E-mail: yu_zhang1225@163.com.
[c] Key Laboratory of Agricultural Environmental Microbiology, Ministry of Agriculture and Rural Affairs, College of Life Sciences, Nanjing Agricultural University, Nanjing, 210095, China.
[d] State Key Laboratory of Materials-oriented Chemical Engineering, College of Biotechnology and Pharmaceutical Engineering, Nanjing Tech University, 30 Puzhu South Road, Nanjing, 211816, China.
[e] School of Chemistry, Centre for Research on Adaptive Nanostructures and Nanodevices (CRANN) and Advanced Materials Bio-Engineering Research Centre (AMBER), Trinity College Dublin, Dublin, D02PN40 Ireland.

Email: bochengqiu@njau.edu.cn and yu_zhang1225@163.com

Experimental Section

Materials and Methods

Preparation of $Pd/Ni(OH)_2/NF$: Typically, commercial NF was sequentially washed using acetone, diluted HCl (3 M), and deionized (DI) water with ultrasound treatment. Then, a piece of NF (5*5 cm) was immersed into a mixed aqueous solution of 180 mL containing 0.5 mg mL^{-1} K_2PdCl_6 and 5 mM NaCl. After immersion for 3 h, the $Pd/Ni(OH)_2/NF$ was taken out from the solution, washed with DI water, and dried at 40 ^oC. The Pd loading density was determined to be 0.20 mg cm^{-2} using ICP-OES. To obtain the optimal Pd loading density, the $Pd/Ni(OH)_2/NF$ with Pd loading densities of 0.12 and 0.31 mg cm^{-2} were prepared as reference samples, using the K_2PdCl_6 solution of 0.25 and 1.0 mg mL^{-1}, respectively. Bare $Ni(OH)_2/NF$ was synthesized with the absence of K_2PdCl_6.

Preparation of TiO_2/TF: Typically, commercial Ti felt (TF) was washed using ethanol and deionized (DI) water with ultrasound treatment. Then, a piece of TF (2.5*2.5 cm) was placed into a 50 mL Teflon autoclave containing 30 mL 1 M NaOH, which was heated at 200 ^oC for 12 h. The TF covered with sodium titanate was taken out from the autoclave, immersed in 0.1 M HCl to exchange Na^+ with H^+, washed using DI water several times, dried at 40 ^oC, and eventually calcinated at 450 ^oC for 1 h in a muffle furnace.

Characterizations

X-ray diffraction (XRD) patterns were collected by using a Rigaku/MiniFlex600 diffractometer with a monochromatic Cu Kα radiation source. Scanning electron microscopy (SEM) and transmission electron microscopy (TEM) images were recorded on a Hitachi Regulus8100 scanning electron microscope and JEOL 2100F transmission electron microscope, respectively. Aberration-corrected scanning transmission electron microscopy (AC-STEM) was done with a FEI Titan G2 60-300 transmission electron microscope with an acceleration voltage of 300 kV. X-ray photoelectron spectroscopy (XPS) measurements were carried out using Thermo Scientific K-Alpha with an aluminum anode (*hv*=1486.6 eV) at 12 kV. Pd loading amount was determined by ICP-OES (Thermo Fisher iCAP PRO). Fourier-transform infrared spectroscopy (FT-IR) was carried out on a FT-IR spectrometer (Thermo Scientific Nicolet iS5) with attenuated total reflection (ATR) model. *In-situ* Raman spectra were collected using a confocal Raman spectrometer (WITec alpha300 R) equipped with a 532 nm excitation wavelength, a laser power of 3 mW, a grating of 1800 grooves mm^{-1}. A ×50 objective (Zeiss) was utilized for focusing. The crystallinity for PLA plastic was estimated by a DSC 3 (Mettler Toledo) with a heating rate of 10 ^oC min^{-1}. The electrooxidation measurements were carried out under pulsed and potentiostatic conditions in a 20 mL electrolyte containing 0.3 M lactic acid and 1.0 M KOH. Note that the time resolution of the Raman spectra (approximately 10 s per spectrum) can not allow us to identify the surface species

during each individual pulse, and thus it only reflects the average state of the catalyst surface. *In-situ* Fourier transform infrared spectroscopy (FTIR) was conducted on an IRTracer-100 FTIR spectrometer equipped with a mercury–cadmium–telluride detector, using silicon as the prismatic window. Before each test, Au film was chemically deposited on the surface of the silicon prism. The catalyst ink (5 mg catalysts into 175 μL DI water and 800 μL ethanol containing 25 μL of 5 wt.% Nafion) was carefully dropped on the surface of the Au film, and the silicon prism deposited with the catalysts served as the working electrode. The Pt foil and Ag/AgCl electrodes were used as the counter and reference electrodes, respectively. The electrolyte for electrochemical reductive amination of pyruvate was 0.2 M H_2SO_4 solution (containing 0.2 M potassium pyruvate and 0.2 M hydroxylamine hydrochloride). The infrared spectra were collected at -0.2 V vs. RHE. The spectra were collected nine times at an electrocatalytic time of 30 min. Before each systemic measurement, the background spectrum of the catalyst electrode was acquired at an open-circuit voltage.

PLA plastic depolymerization: 1.6 g PLA plastic (commercial granule (3 mm, molecule weight ~80000), PLA straw, PLA cup, or PLA folk) was added into 60 M 1.3 M KOH solution, and after stirring for 12 h at 80 ^oC, the PLA plastic was completely depolymerized into lactic acid monomer constitute (lactic acid exists as lactate under alkaline condition), and the PLA hydrolysate can be used as the feedstocks for the subsequent pulsed electrooxidation.

Electrochemical measurements: 1) The pulsed electrooxidation of lactate into pyruvate was conducted using PLA hydrolysate (0.3 M lactate and 1.0 M KOH) and 1.0 M KOH solution as anode and cathode electrolytes, respectively, in a membrane electrode assembly (MEA) electrolyser. The MEA reactor was comprised of metal housings, gaskets, as-made catalysts (2*2 cm $Pd/Ni(OH)_2/NF$ as both anode and cathode), and anion-exchange membrane (AEM, Fuma FAA-PK-130). 2) The electroreduction of pyruvate into alanine was performed in a MEA cell, in which a piece of proton-exchange membrane (PEM, Nafion NRE-117), TiO_2/TF (2*2 cm), and commercial IrO_2 supported by TF (IrO_2/TF, 2*2 cm) were used as a separator, a cathodic electrode, and an anode electrode, respectively. 15 mL 0.2 M H_2SO_4 solution containing 0.2 M lactate and 0.2 M NH_2OH (nitrogen source) was used as cathode electrolyte, while 15 mL 0.5 M Na_2SO_4 was utilized as anode electrolyte.

Calculation equations for FE, selectivity, and yield to target products

$$\text{Pyruvate FE}(\%) = \frac{2 * 96485.3 * \text{Moles of the obtained pyruvate}}{\text{Totally passed charges}} * 100\%$$

$$\text{Pyruvate selectivity}\ (\%) = \frac{\text{Moles of the obtained pyruvate}}{\text{Moles of the consumed lactate}} * 100\%$$

$$\text{Pyruvate yield (\%)} = \frac{\text{Moles of the obtained pyruvate}}{\text{The initial lactate}} * 100\%$$

$$\text{Alanine FE(\%)} = \frac{4 * 96485.3 * \text{Moles of the obtained alanine}}{\text{Totally passed charges}} * 100\%$$

$$\text{Alanine yield (\%)} = \frac{\text{Moles of the obtained alanine}}{\text{The initial pyruvate}} * 100\%$$

Calibration of electrochemical active surface area

The Cu underpotential deposition method was employed to determine the electrochemical active surface area of noble-metal-based materials.[1-2] Typically, all the calibration tests were carried out in N_2 saturated electrolyte containing 0.5 M Na_2SO_4 and 20 mM $CuSO_4$. Before Cu deposition, the catalysts were scanned (5 mV s^{-1}) from 0 to 1.1 V for several cycles in 0.5 M Na_2SO_4 as the background. During the CV scan, the Cu stripping started at 0.5 and 1.1 V with an obvious anodic peak. The number of active Pd sites can be associated with the Cu stripping charge (Q_{Cu}) subtracting the capacity influence determined in 0.5 M $NaSO_4$ solution. Consequently, the ECSA can be calibrated as follows: $ECSA = Q_{CU} /(M_{metal} * 424\ \mu C\ cm^{-2})$, where M_{metal} is the Pd loading density.

Product purification

1) Pyruvate purification: the post-reaction electrolyte was adjusted with 3 M HCl to pH value of 5, which was then concentrated at 40 ^oC under vacuum to viscous state. Ethanol was then added to initiate the product precipitation from the solution, and the crystalline slurry (*i.e.*, pyruvate) was filtered and dried at 40 ^oC under vacuum for overnight. 2) Alanine purification: the post-reaction electrolyte, including alanine, $NH_2OH{\cdot}HCl$, and K_2SO_4, was concentrated to viscous state, and acetic acid was then introduced to separate K_2SO_4 from solution. Alanine was finally obtained by using rotatory evaporation for acetic acid and $NH_2OH{\cdot}HCl$ removal. Note that the K_2SO_4 in the post-reaction electrolyte originated from potassium pyruvate and H_2SO_4 that were used as reactant and electrolyte.

Product analysis

The concentrations of lactate (reactant), pyruvate (product), and acetate (byproduct) from the pulsed electrochemical oxidation of lactate were monitored by HPLC (Waters2489) equipped with an Agilent C18 column and an ultraviolet-visible detector. The mobile phase was consisted of 10 mM NaH_2PO_4 (95 vol%) and methanol (5 vol%) with a flow rate of 1.0 mL/min. The concentrations of lactate and oxime in the post-reaction electrolyte collected from the cathodic chamber were analyzed using HPLC with an Agilent SB-AQ column and an ultraviolet-visible detector, and the mobile phase was consisted of 10 mM NaH_2PO_4 (95 vol%) and methanol (5

vol%) with a flow rate of 0.8 mL/min. The qualitative analysis for the alanine product was carried out using ^{1}H nuclear magnetic resonance (NMR; AVANCE III 400 MHz, Bruker) spectra with maleic acid as internal standard. ^{1}H and ^{13}C nuclear magnetic resonance spectra were used to confirm the chemical structure of the obtained product. The generated hydrogen was analyzed using gas chromatography (GC, FULI INSTRUMENTS GC9790Plus) equipped with a thermal conductivity detector and a molecular sieve column with Ar as the carrier gas.

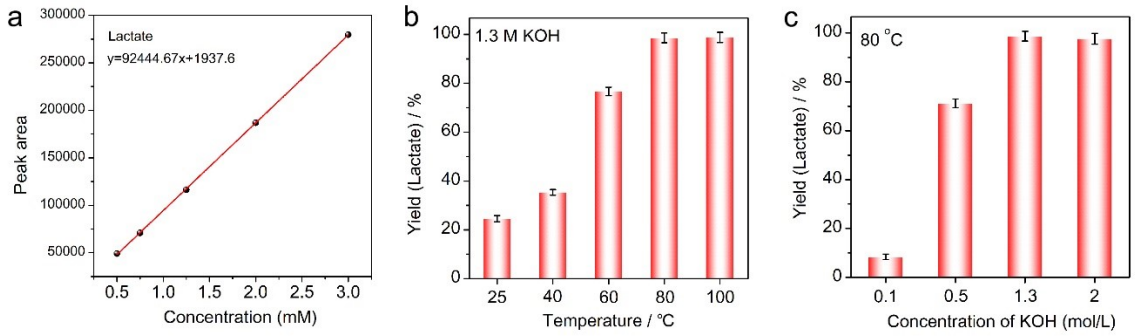

Fig. S1 (a) Calibration curve of lactate. (b,c) The effects of operation temperature (b) and KOH concentration (c) on the lactate yield. Reaction conditions: 1.63 g commercial PLA granule (size: 3 mm, molecule weight: ~80000, PLA content: >99%), 60 mL KOH solution, 12 h.

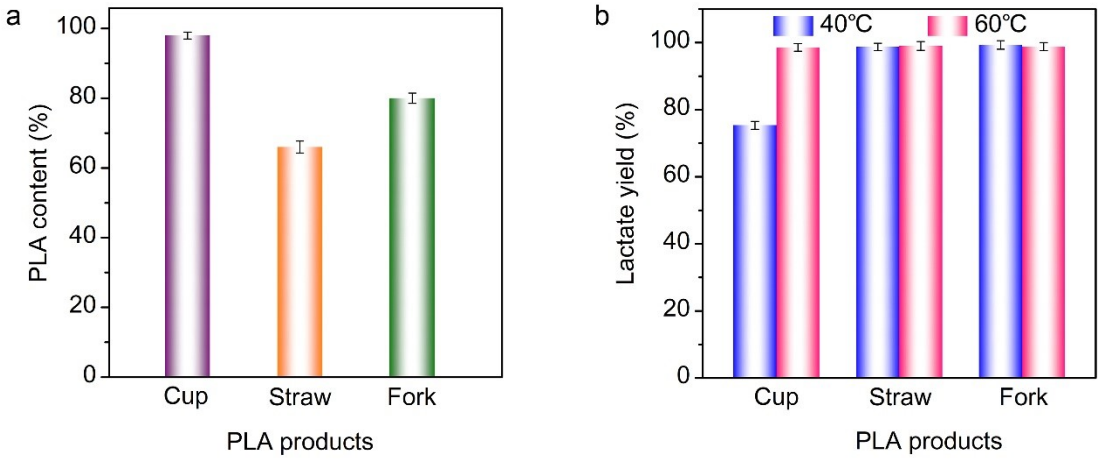

Fig. S2 (a) PLA content in post-consumer PLA products: including cup, straw, and fork. (b) The effect of reaction temperature on depolymerization of different post-consumer PLA products. Reaction conditions: 1.63 g PLA product, 60 mL 1.3 M KOH solution, 12 h.

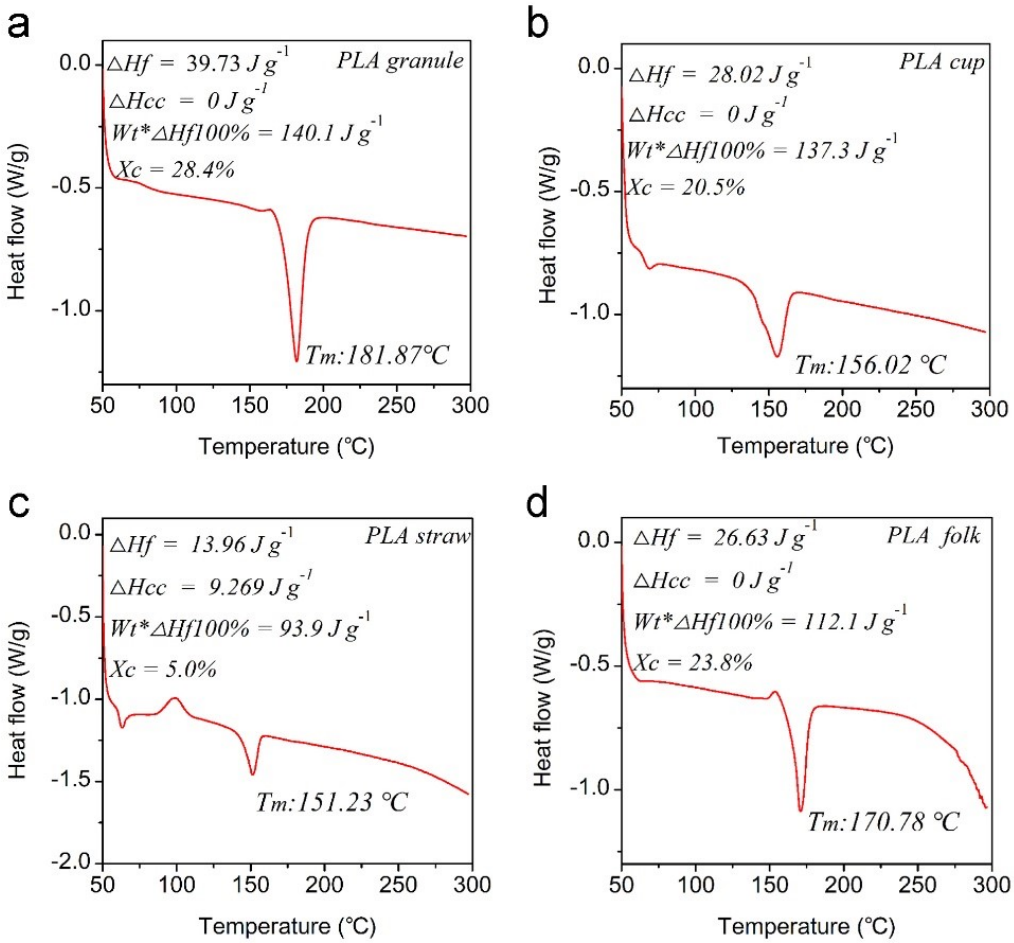

Fig. S3 Crystallinity measurements of commercial PLA granule (a), PLA cup (b), PLA straw (c), and PLA folk (d) using differential scanning calorimetry (DSC) with a heating rate of 10 °C min^{-1}. Percentage of crystallinity (*Xc*) was calculated using the equation: $Xc(\%) = 100\%*(\Delta Hf\text{-}\Delta Hcc)/(Wt*\Delta Hf100\%)$, where ΔHf is the melting enthalpy that can be calculated by integrating the endothermic melting peak, ΔHcc is the enthalpy of cold crystallization and determined by integrating the exothermic cold crystallization peak, Wt is the weight fraction of polyester in the plastic (*Wt* is taken as 100%, 98%, 66%, and 80% for PLA granule, cup, straw, and folk, respectively), and $\Delta Hf100\%$ is the melting enthalpy for a fully crystalline polymer and taken as 140.1 J g^{-1}.[3] To improve the rigidity and thermal stability, PLA folks typically contain $CaCO_3$ and talc as additives, which thus increases the crystallinity of the PLA folk.

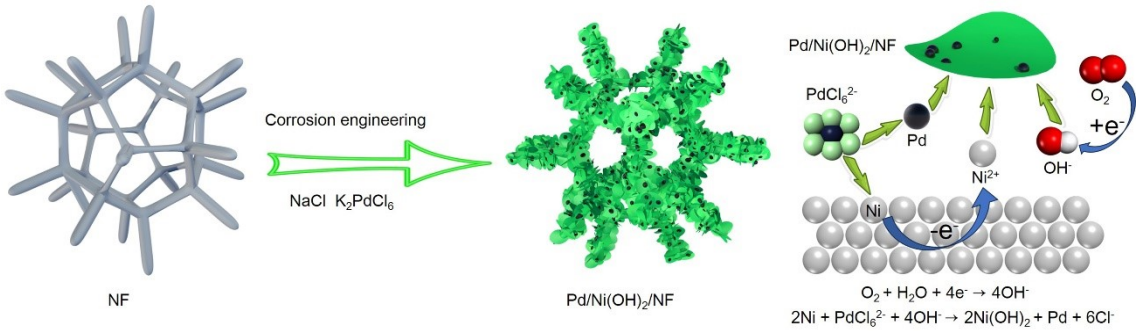

Fig. S4 Schematic illustration of $Pd/Ni(OH)_2/NF$ preparation.

Typically, the favorable thermodynamic process ($E_{(PdCl6)2-/Pd}>E_{Ni(OH)2/Ni}$) allows a spontaneous redox reaction between $(PdCl_6)^{2-}$ ion and Ni foam to form metallic Pd and Ni^{2+}.[4-5] In parallel, the dissolved oxygen undergoes a reduction reaction ($O_2 + 2H_2O + 4e^- \rightarrow 4OH^-$) to generate hydroxide ions (OH^-), thus leading to the formation of $Ni(OH)_2$ accompanied by effective loading of Pd nanoparticles on $Ni(OH)_2$ nanosheets. Note that NaCl is utilized to promote the corrosion process.

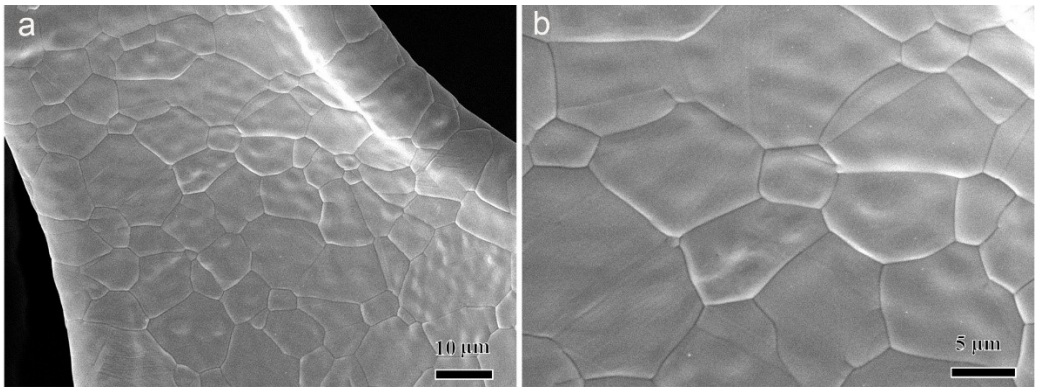

Fig. S5 (a,b) SEM image of bare NF.

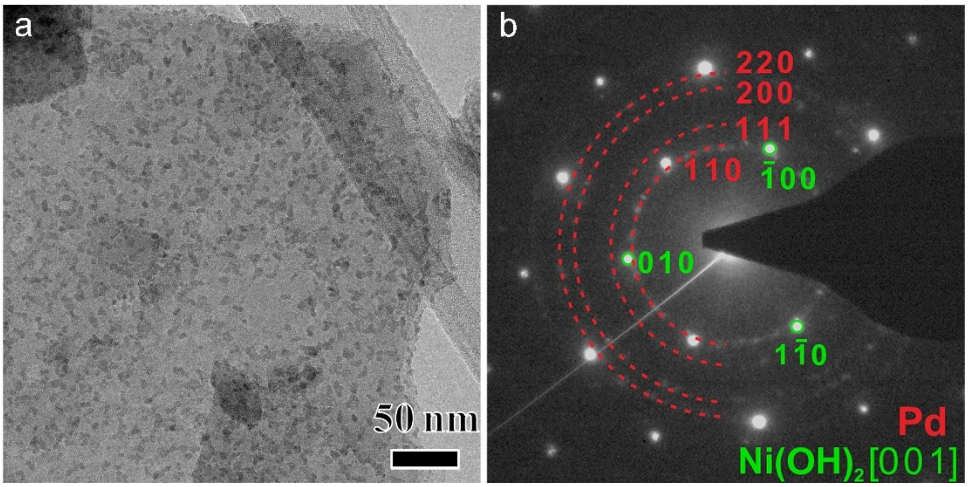

Fig. S6 (a) TEM images of Pd/Ni(OH)$_2$/NF and (b) the corresponding selected area electron diffraction (SAED) pattern. The SAED pattern shows the coexistence of Pd and Ni(OH)$_2$.

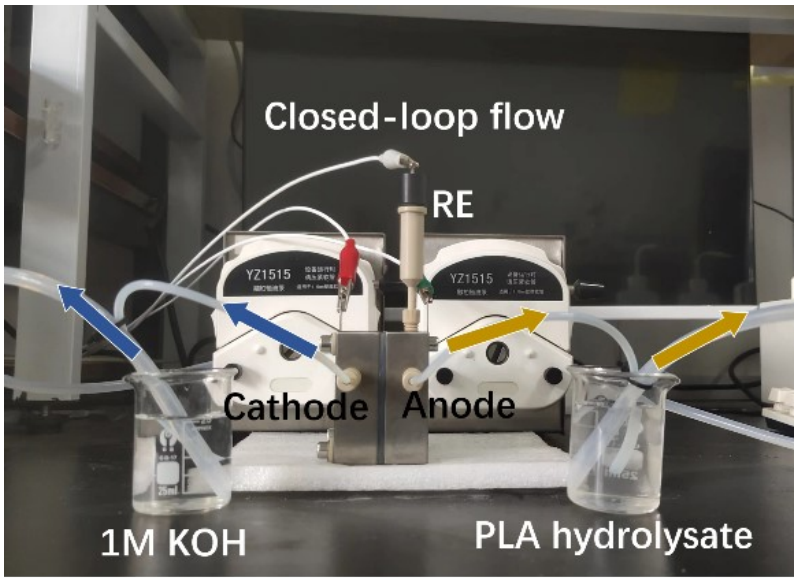

Fig. S7 The photograph of the MEA reactor for electrooxidation of lactate by feeding PLA hydrolysate (0.3 M lactate and 1 M KOH) and 1 M KOH as anolyte and catholyte, respectively. Note that the Pd/Ni$(OH)_2$/NF is used as both anode and cathode, and Hg/HgO was reference electrode (RE). Note that we employed the closed-loop flow to improve the conversion rate of lactate, and the flow rate for both anolyte and catholyte is controlled to be 0.6 mL min^{-1}.

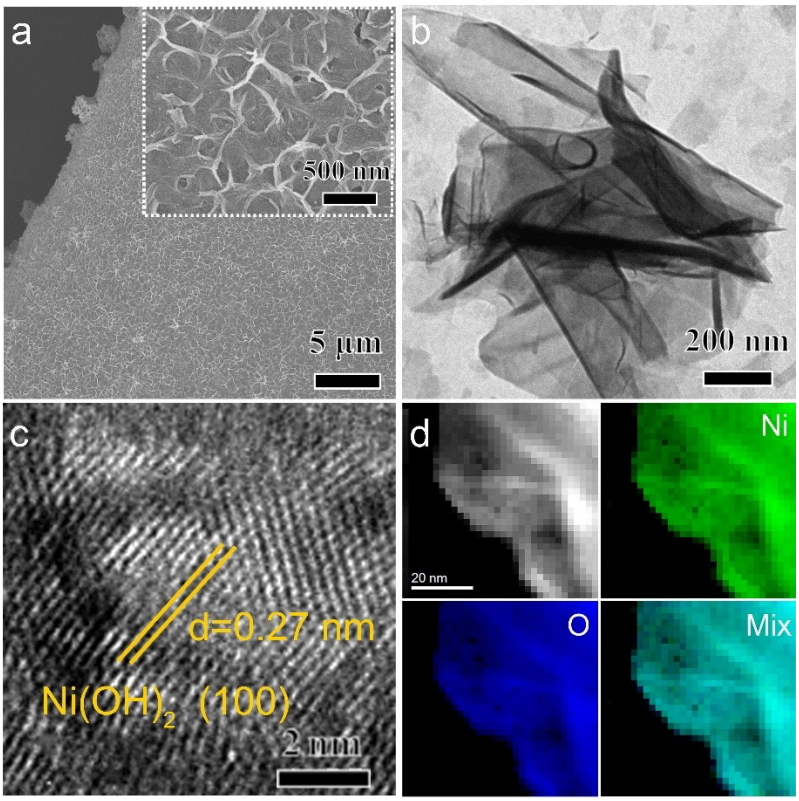

Fig. S8 (a) SEM images, (b) TEM image of $Ni(OH)_2$/NF, (c) HRTEM image, and (d) element mapping of $Ni(OH)_2$/NF.

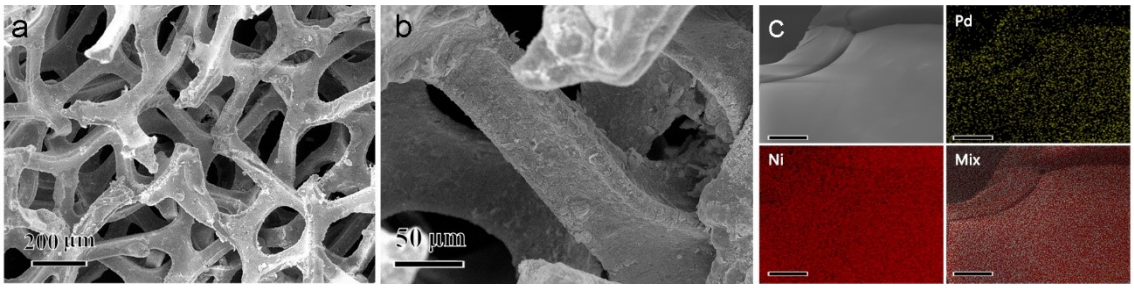

Fig. S9 (a,b) SEM images and (c) the corresponding element mapping of Pd/NF (the scale bar is 5 μm), and the loading density of Pd on NF is determined to be approximately 0.19 mg cm^{-2} using inductively coupled plasma optical emission spectrometer (ICP-OES), close to that on Pd/$Ni(OH)_2$/NF (0.2 mg cm^{-2}).

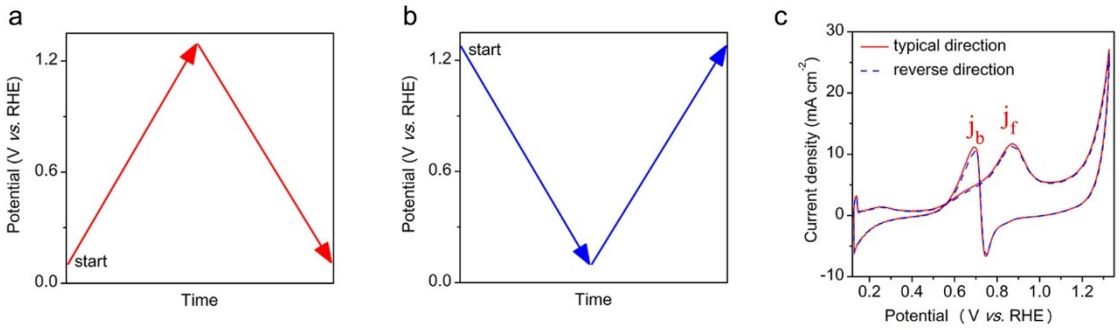

Fig. S10 Lactate electrooxidation mechanism. (a) Typical direction, (b) reverse direction, and (c) CV curves on Pd/Ni(OH)$_2$/NF (red line: typical direction; blue dashed line: reverse direction).

The typical direction (Fig. S10a) means that the CV curve is recorded from forward scan (0-1.3 V vs RHE) to backward scan (1.3-0 V vs RHE). The reverse direction (Fig. S10b) means that the CV curve is recorded from backward scan (1.3-0 V vs RHE) to forward scan (0-1.3 V vs RHE). Note that if j_b present in CV with typical direction is caused by forward scan residual intermediate, the reverse-direction forward scan features should be different from that in the typical-direction backward scan. However, the obtained CV curves are independent on the scan direction and almost identical (Fig. S10c), thus indicating that j_b is not related to CO poisoning but rather to freshly chemisorbed lactate oxidation, which agrees with the previous results observed for methanol oxidation over Pt-based catalysts.[6]

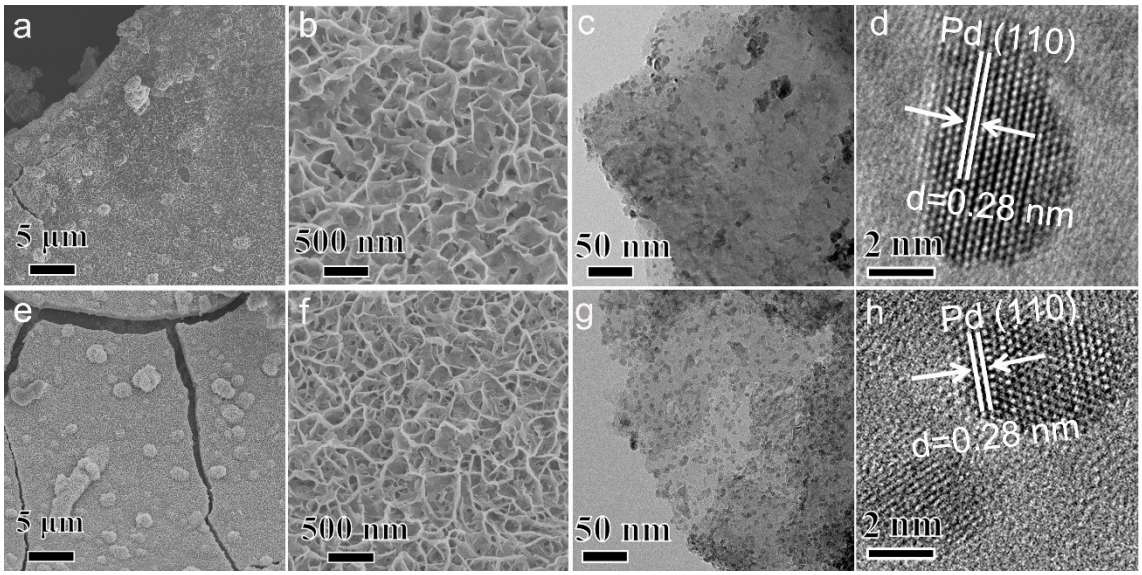

Fig. S11 SEM and TEM images of Pd/Ni$(OH)_2$/NF with different Pd loading densities: (a-d) 0.12 mg cm^{-2} and (e-h) 0.31 mg cm^{-2}.

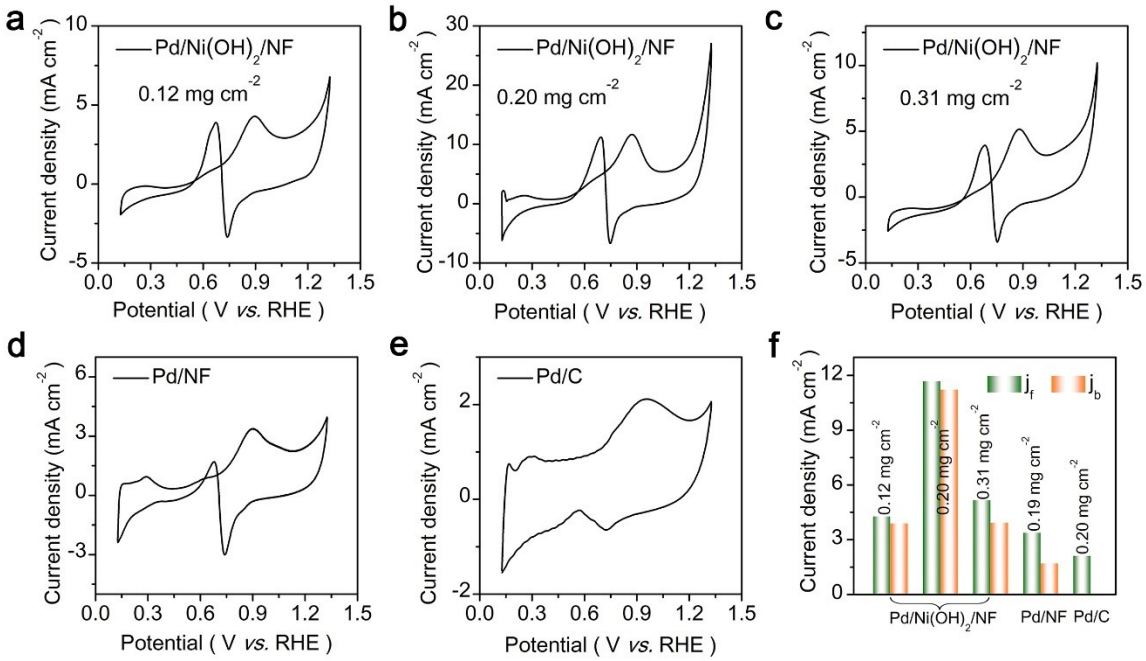

Fig. S12 CV profiles of $Pd/Ni(OH)_2/NF$ with different Pd loading densities, Pd/NF, and Pd/C (supported by NF) recorded at a scan rate of 5 mV s^{-1} in 0.3 M lactate and 1 M KOH: (a) $Pd/Ni(OH)_2/NF$ with Pd loading density of 0.12 mg cm^{-2}, (b) $Pd/Ni(OH)_2/NF$ with Pd loading density of 0.20 mg cm^{-2}, (c) $Pd/Ni(OH)_2/NF$ with Pd loading density of 0.31 mg cm^{-2}, (d) bare Pd/NF with Pd loading density of 0.20 mg cm^{-2}, (e) commercial Pd/C (supported by NF) with Pd loading density of 0.20 mg cm^{-2} and (f) the j_f and j_b values of various samples. Note that j_f and j_b mean the peak current density in the forward and backward scans, respectively.

With the same Pd loading density (~0.20 mg cm^{-2}), $Pd/Ni(OH)_2/NF$ shows the larger j_f value, corresponding to the higher activity toward lactate oxidation, with respect to Pd/NF and Pd/C. Note that the lactate oxidation peak on Pd/C in the backward scan is absent. Meanwhile, $Pd/Ni(OH)_2/NF$ with Pd loading density of 0.20 mg cm^{-2} allows the best activity among all the $Pd/Ni(OH)_2/NF$ catalysts with different Pd loading densities, indicating that the Pd loading density of 0.20 mg cm^{-2} is optimal.

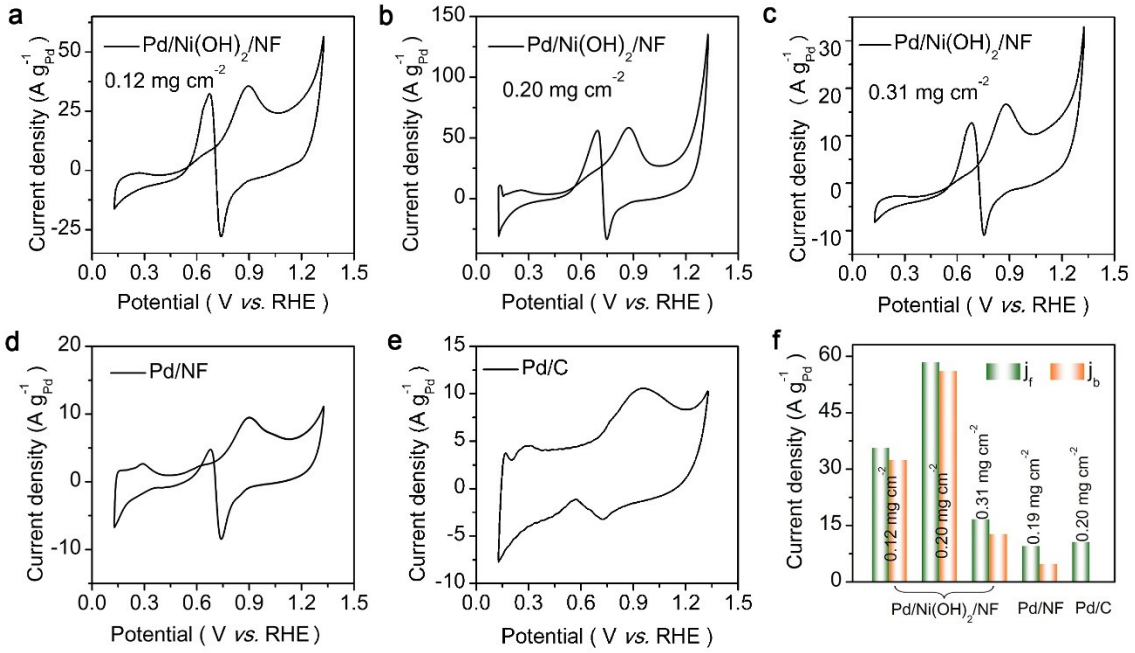

Fig. S13 CV curves of various samples normalized by their corresponding mass loadings: (a) $Pd/Ni(OH)_2/NF$ with Pd loading density of 0.12 mg cm^{-2}, (b) $Pd/Ni(OH)_2/NF$ with Pd loading density of 0.20 mg cm^{-2}, (c) $Pd/Ni(OH)_2/NF$ with Pd loading density of 0.31 mg cm^{-2}, (d) bare Pd/NF with Pd loading density of 0.20 mg cm^{-2}, (e) commercial Pd/C (supported by NF) with Pd loading density of 0.20 mg cm^{-2} and (f) the j_f and j_b values of various samples.

When the catalytic activities over various catalysts were normalized by their corresponding Pd mass loadings, the $Pd/Ni(OH)_2/NF$ catalyst with Pd loading density of 0.2 mg cm^{-2} still enables the best performance for lactate oxidation, with the highest j_f anf j_b values.

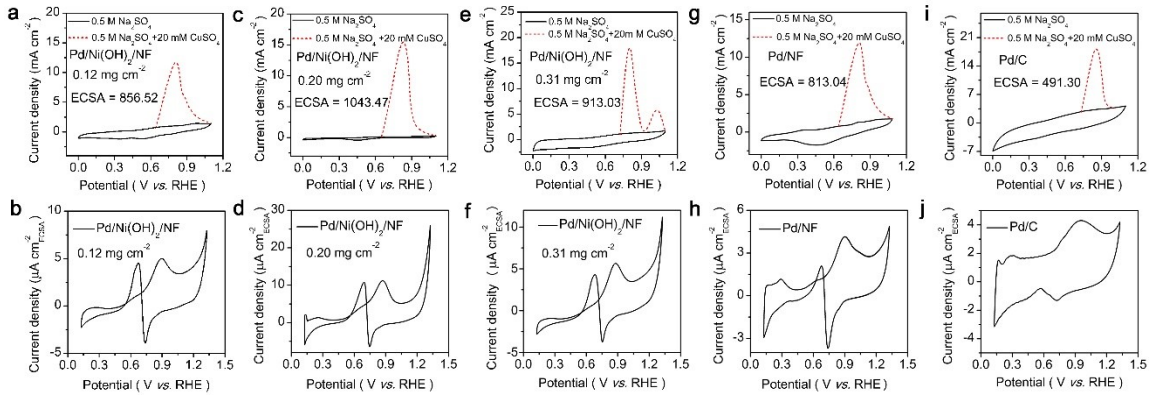

Fig. S14 Electrochemical active surface area (ECSA) measurements of various samples using copper underpotential deposition on Pd and their corresponding CV curves normalized by the ECSA values: (a,b) Pd/Ni(OH)$_2$/NF with Pd loading density of 0.12 mg cm^{-2}, (c,d) Pd/Ni(OH)$_2$/NF with Pd loading density of 0.20 mg cm^{-2}, (e,f) Pd/Ni(OH)$_2$/NF with Pd loading density of 0.31 mg cm^{-2}, (g,h) bare Pd/NF with Pd loading density of 0.20 mg cm^{-2}, and (i,j) commercial Pd/C (supported by NF) with Pd loading density of 0.20 mg cm^{-2}.

To further compare the intrinsic activity, we normalized the catalytic activity for lactate oxidation over various catalysts by their corresponding ECSA values. Notably, the Pd/Ni(OH)$_2$/NF catalyst with Pd loading density of 0.2 mg cm^{-2} still delivers the highest activity in terms of j_f and j_b (Table S1).

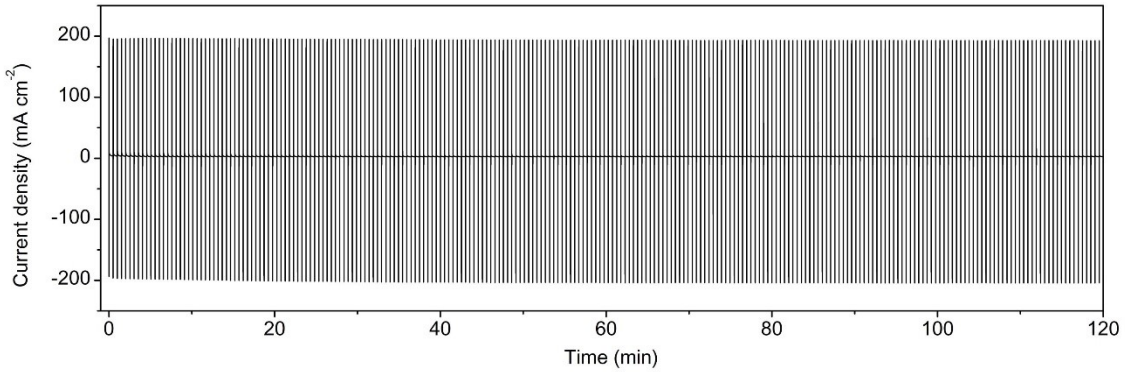

Fig. S15 Pulsed response for lactate electrooxidation over Pd/Ni(OH)$_2$/NF at 0.90 V (E_{high}) for 0.2 s followed by 0.73 V (E_{low}) for 30 s, repeating this sequence for 120 min.

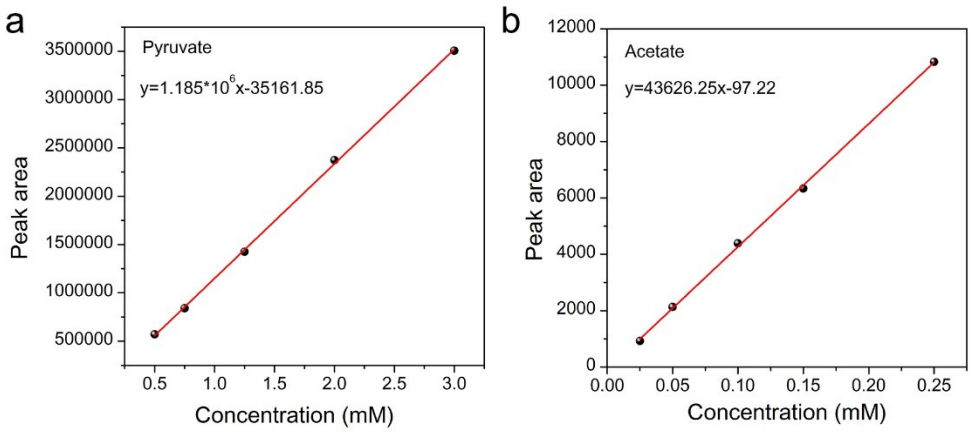

Fig. S16 Calibration curves of pyruvate (a) and acetate (b).

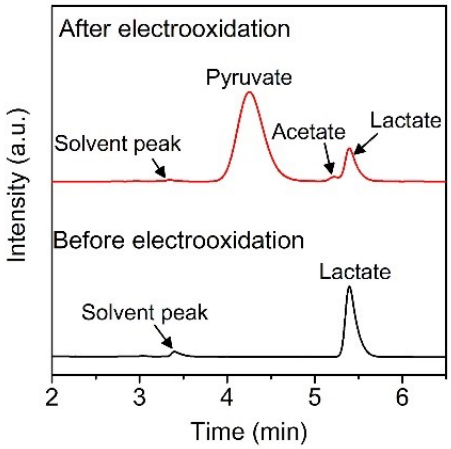

Fig. S17 HPLC spectra of anodic electrolyte before and after 8-h pulsed electrooxidation.

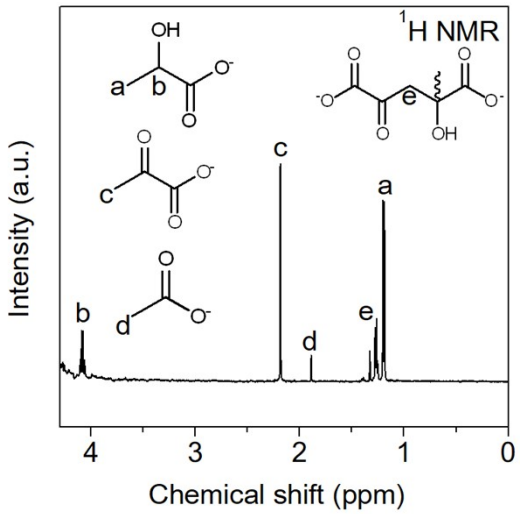

Fig. S18 ^{1}H NMR of anodic electrolyte after 8-h pulsed electrooxidation. With the exception of acetate byproduct, the oligomer, namely 4-hydroxy-4-methyl-2-oxoglutaric acid, was evolved during the lactate oxidation process.[7] According to the previous report, pyruvate accumulation will lead to the formation of oligomer.[8] The pyruvate product was qualified by HPLC in our work (the pyruvate FE was calculated based on the HPLC result), however, the generated oligomer could not be detected by HPLC, which thus leads to the pyruvate FE reduction (Fig. 3f).

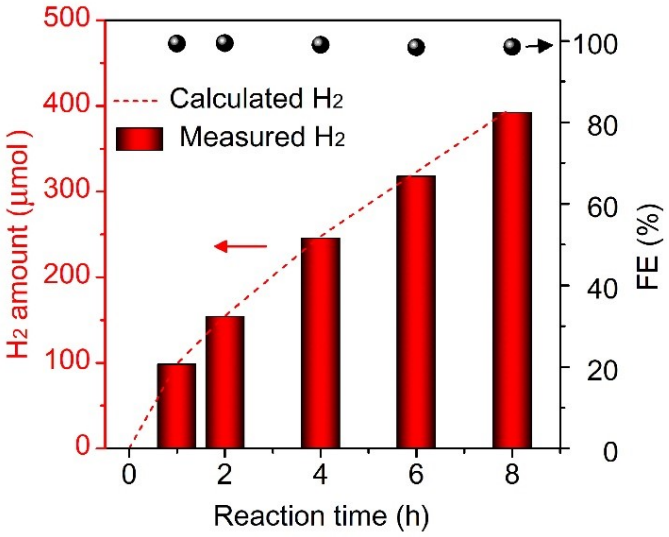

Fig. S19 H_2 amounts collected from the cathode chamber and the theoretical calculated H_2 production, and the FE for cathodic hydrogen evolution.

In parallel with the anodic electrooxidation of pyruvate, the measured quantity of H_2 evolved from cathode chamber is approaching to the theoretical calculated H_2, indicating the near-unity FE for hydrogen evolution.

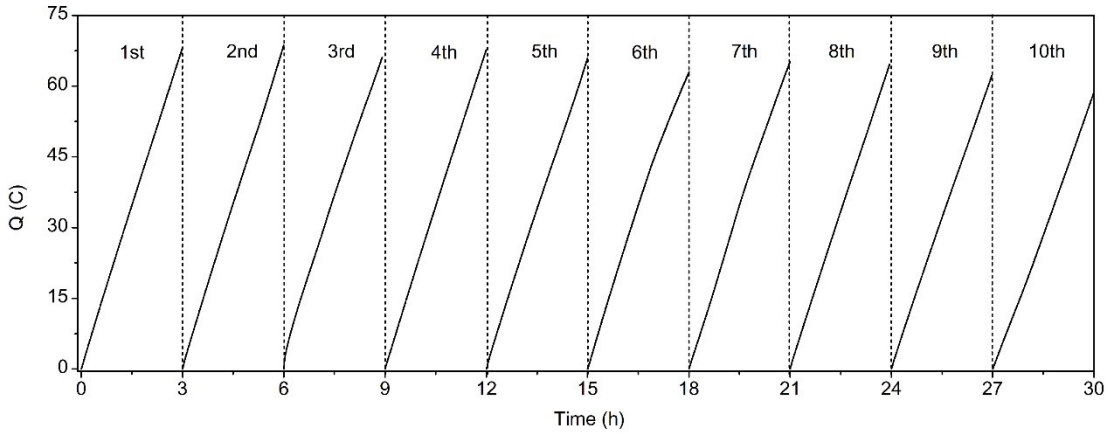

Fig. S20 The accumulated charge in ten repeated cycles for pulsed electrooxidation of pyruvate (each cycle lasts for 3 h). Reaction conditions: Pd/Ni$(OH)_2$/NF (2*2 cm) as anode and cathode, 2.5 mL 1 M KOH solution containing 0.3 M lactate as anolyte, flow rate of 0.6 mL, the anolyte was refreshed after each cycle.

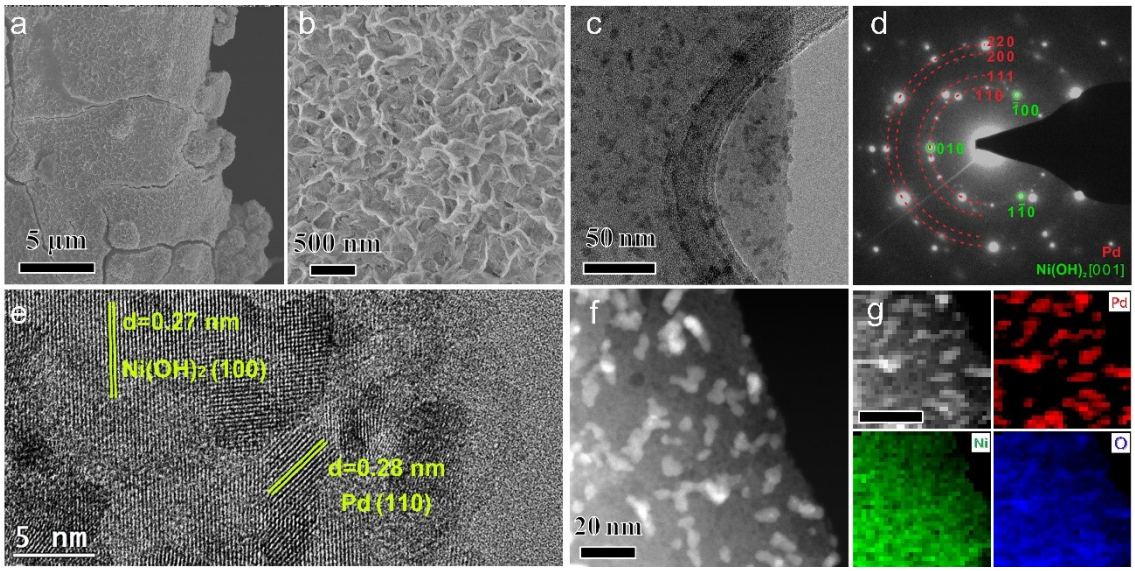

Fig. S21 Morphology characterizations of the recovered catalyst. (a,b) SEM images, (c) TEM image and (d) its corresponding SAED pattern, (e) HRTEM image, (f) STEM image, and (g) element mapping (the scale bar is 20 nm).

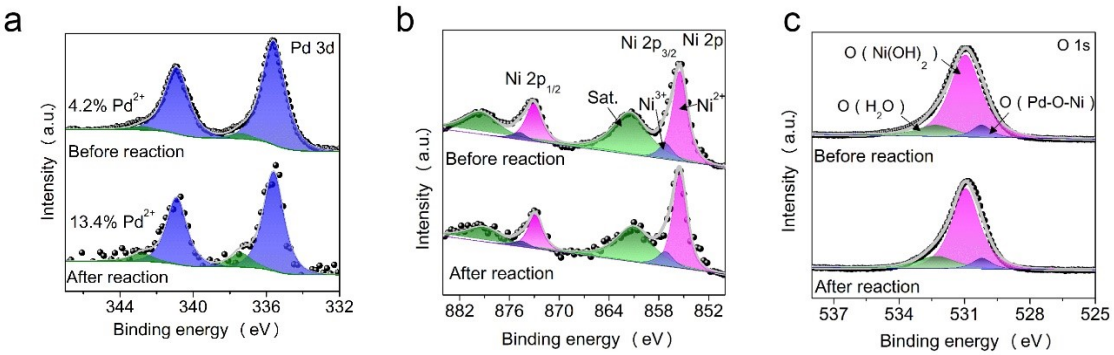

Fig. S22 XPS spectra of Pd/Ni(OH)$_2$/NF before and after pulsed electrooxidation: (a) Pd 3d, (b) Ni 2p, and (c) O 1s.

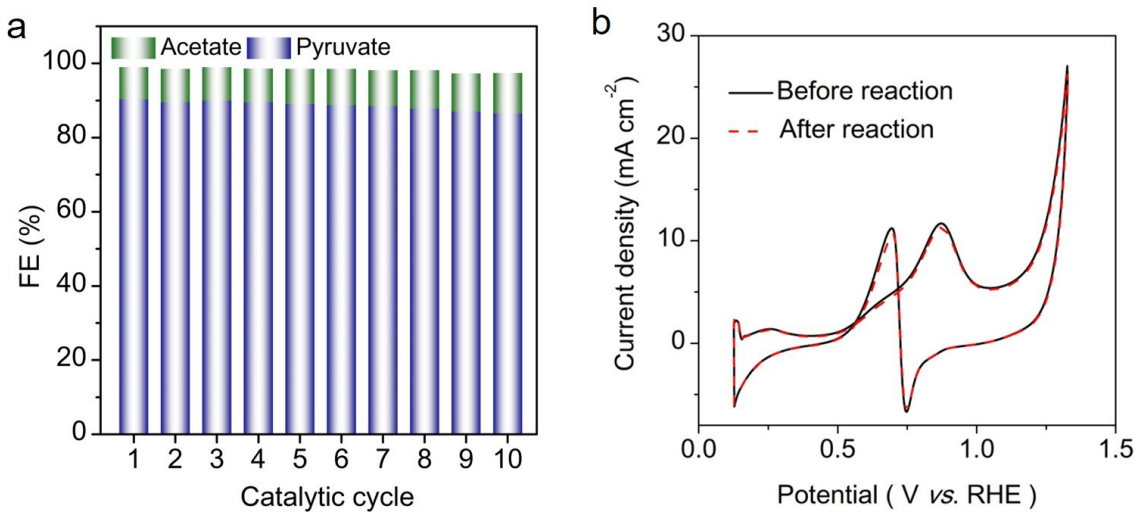

Fig. S23 (a) Repeated catalytic cycles for lactate electrooxidation in impurity-containing PLA hydrolysate and each cycle lasts for 3 h. (b) The CV scan comparison over the fresh and recovered catalysts.

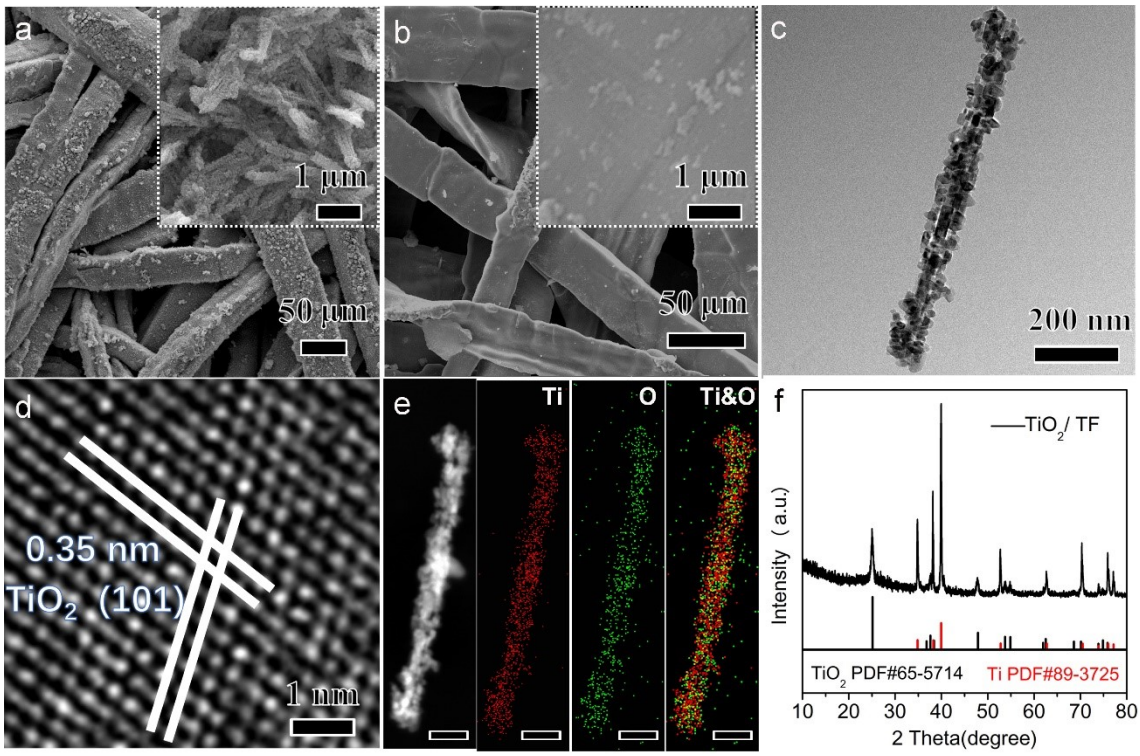

Fig. S24 (a) SEM images of TiO_2/TF. (b) SEM images of bare TF. (c) TEM image, (d) HRTEM image, (e) element mapping (the scale bar is 100 nm), and (f) XRD pattern of TiO_2/TF.

The SEM image of TiO_2/TF (Fig. S22a), compared with that of bare TF (Fig. S22b), shows that TiO_2 nanorods are grown throughout the entire TF substrate. TEM observation (Fig. S22c) confirms the nanorod structure of TiO_2. HRTEM image (Fig. S22d) displays two sets of lattice fringes with spacing of 0.35 nm, corresponding to (101) plane of TiO_2.[9] Element mapping (Fig. S22e) and XRD pattern (Fig. S22f) collectively reveal the successful preparation of TiO_2 nanorods.

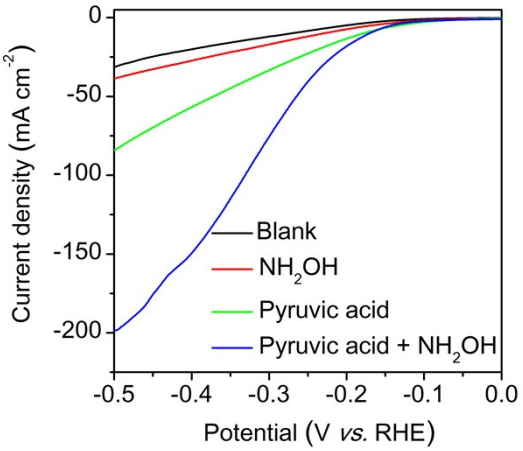

Fig. S25 Polarization curves over TiO_2/TF recorded in 0.2 M H_2SO_4 (black line), 0.2 M H_2SO_4 + 0.2 M NH_2OH (red line), 0.2 M H_2SO_4 + 0.2 M pyruvic acid (green line), and 0.2 M H_2SO_4 + 0.2 M NH_2OH + 0.2 M pyruvic acid (blue line) at a scan rate of 5 mV s^{-1}.

The polarization curve recorded in 0.2 M H_2SO_4 and 0.2 M NH_2OH shows an insignificant change relative to that recorded in 0.2 M H_2SO_4, implying that the reaction is currently dominated by hydrogen evolution reaction (HER). When the reaction is carried out in the presence of 0.2 M H_2SO_4 and 0.2 M pyruvic acid, the measured polarization curve is attributed to HER and reduction of pyruvic acid. Upon the addition of NH_2OH, the substantially improved activity is caused by the reduction of pyruvic oxime.

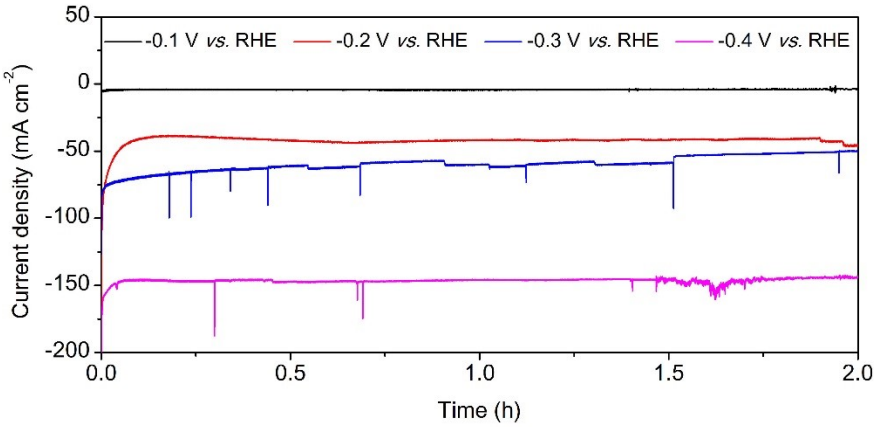

Fig. S26 Chronoamperometric tests over TiO_2/TF recorded at various potentials for 2 h measured at room temperature.

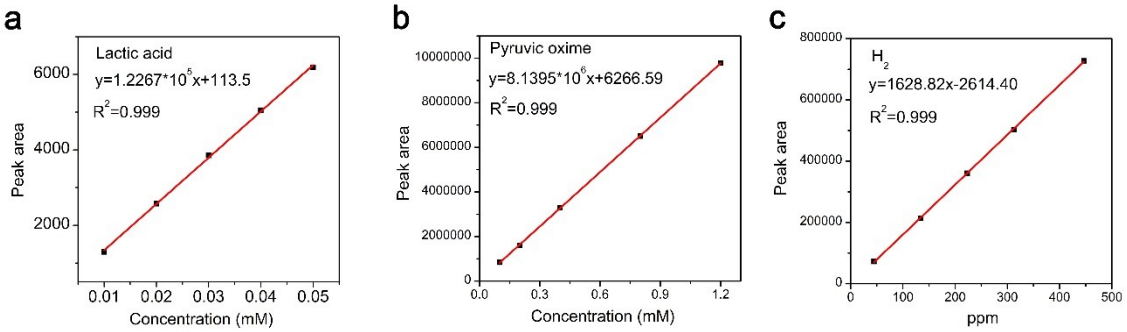

Fig. S27 Calibration curves of lactic acid (a), oxime (b), and H_2 (c). Note that the concentrations of both lactic acid (byproduct) and pyruvic oxime (reactant) were monitored by HPLC, and the gaseous byproduct (hydrogen) was analyzed by gas chromatography (GC).

When NH_2OH as nitrogen source was introduced, most of pyruvic acid reactant was spontaneously converted into pyruvic oxime, and minor of pyruvic acid left in the cathodic electrolyte was reduced into lactic acid during electrochemical transformation. H_2 was evolved from water reduction, which is a competitive process for electrochemical reductive amination of pyruvate into alanine.

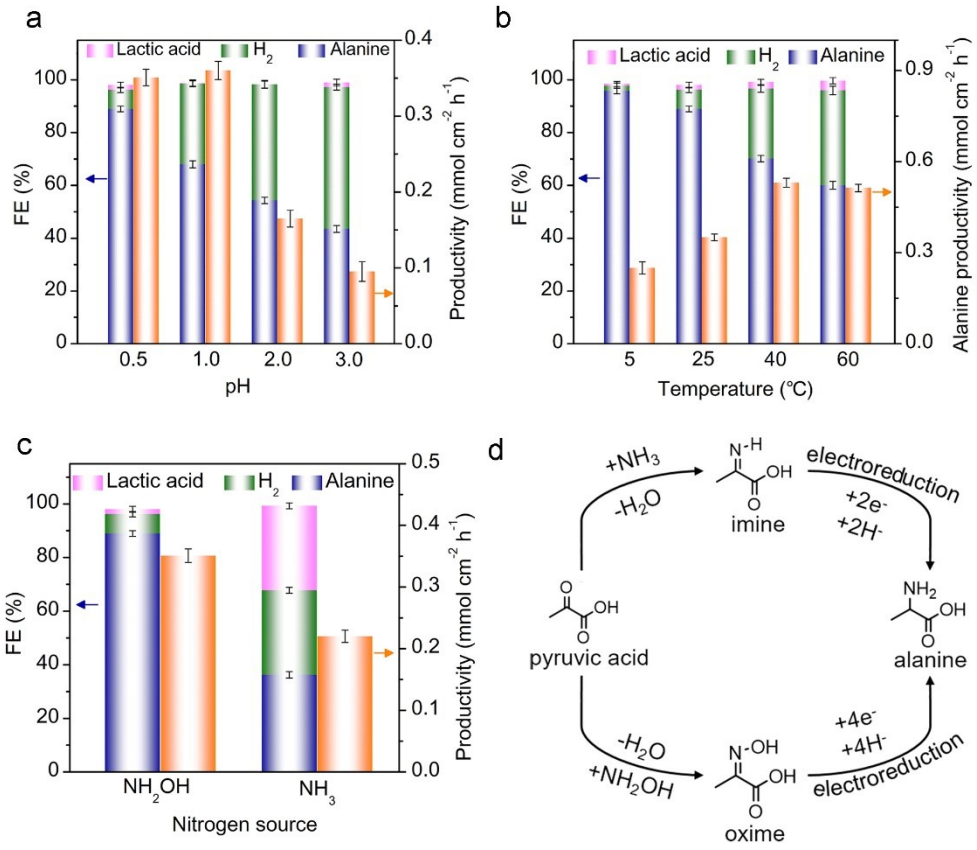

Fig. S28 The effects of (a) electrolyte pH (25 °C and NH_2OH as nitrogen source), (b) temperature (pH=1 and NH_2OH as nitrogen source), and (c) nitrogen source (25 °C and pH=1) on the selectivity and productivity to alanine. (d) Illustration of electrochemical routes to alanine via oxime and imine intermediates using NH_2OH and NH_3 as nitrogen sources, respectively.

We investigated the effects of electrolyte pH, reaction temperature, and nitrogen source on the catalytic performance. The pH range is controlled to be lower than 3, as the protonation of pyruvic oxime occurs at the pH lower than 3 (the pK_a for the oxime protonation is approximately 1.3).[10] When the pH value is close to 0.5, the TiO_2/TF electrode shows the highest FE and productivity to alanine (Fig. S28a). The electrochemical reduction amination reaction carried out at low temperature (5 °C) realizes a highest FE to alanine but is not economically competitive, and considering that a temperature increase renders the competitive HER favorable over TiO_2/TF (Fig. S28b), the temperature of 25 °C (*i.e.*, room temperature) is therefore suitable. Given that the fact that pyruvic oxime undergoes the hydrolysis into pyruvic acid and NH_2OH upon improving temperature under acidic conditions,[11] a temperature increase may induce the reduction of the generated pyruvic acid, which agrees with the results that the FE to lactate slightly improves with the temperature increasing (Fig. S28b). When NH_3 as nitrogen source is introduced, the FE to alanine is about 36%, much lower than that (89%) using NH_2OH as nitrogen source (Fig. S28c). Note that the pathway for alanine production using NH_3 as nitrogen source is based on the protonation of imine (Fig. S28d).

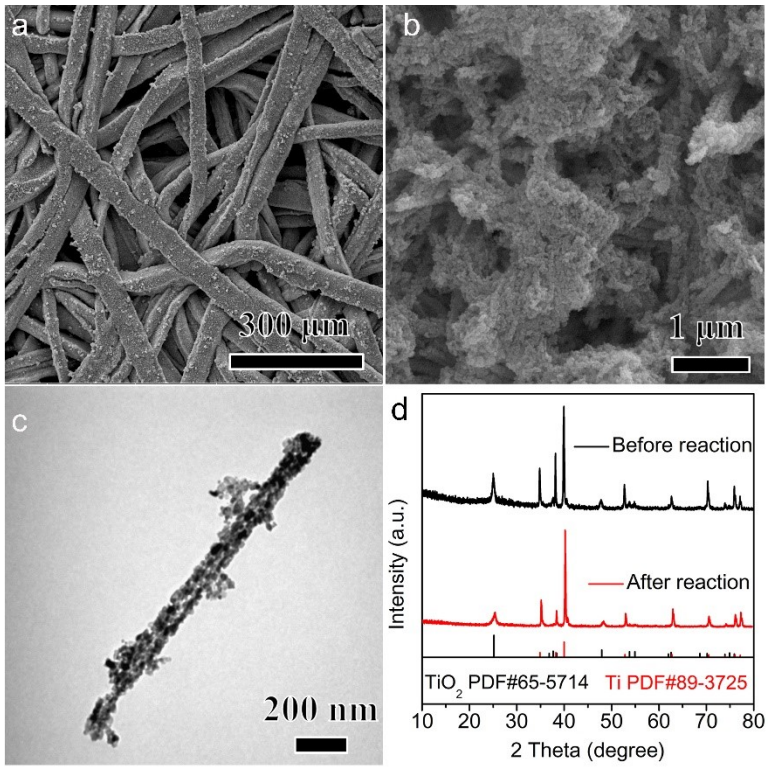

Fig. S29 (a,b) SEM images, (c) TEM image, and (d) XRD patterns of the recovered TiO_2/TF catalyst.

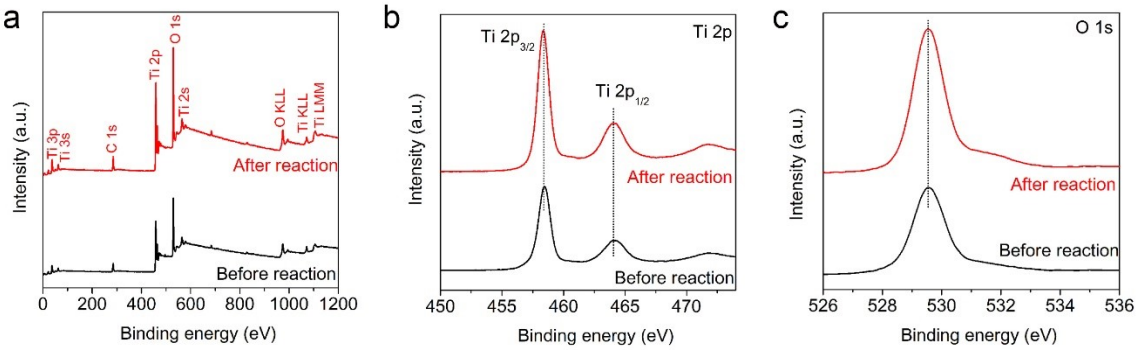

Fig. S30 XPS spectra of the TiO_2/TF before and after electrochemical reductive amination: (a) survey spectra, (b) Ti 2p, and (c) O 1s.

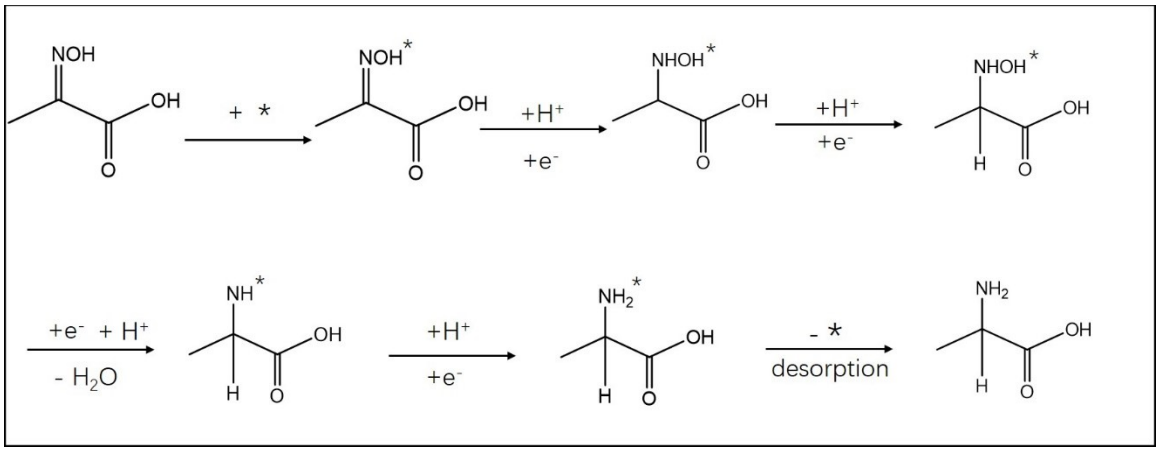

Fig. S31 Alanine production via a hydroxylamine intermediate pathway.

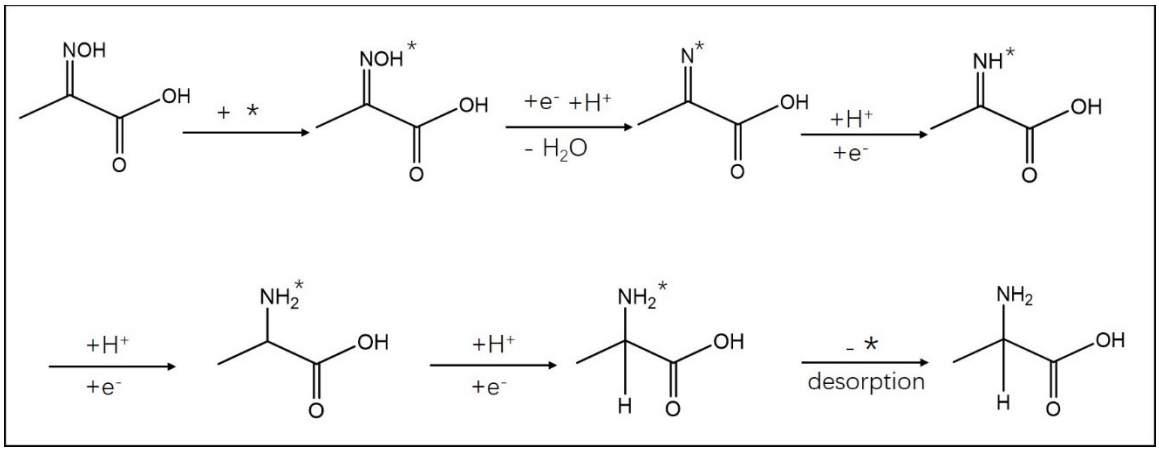

Fig. S32 Alanine production via an imine intermediate pathway.

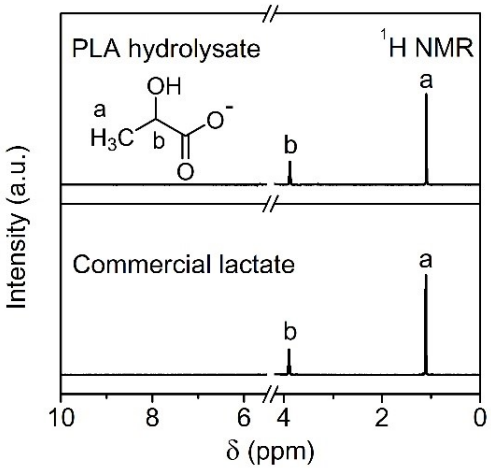

Fig. S33 ^{1}H NMR spectra of PLA hydrolysate.

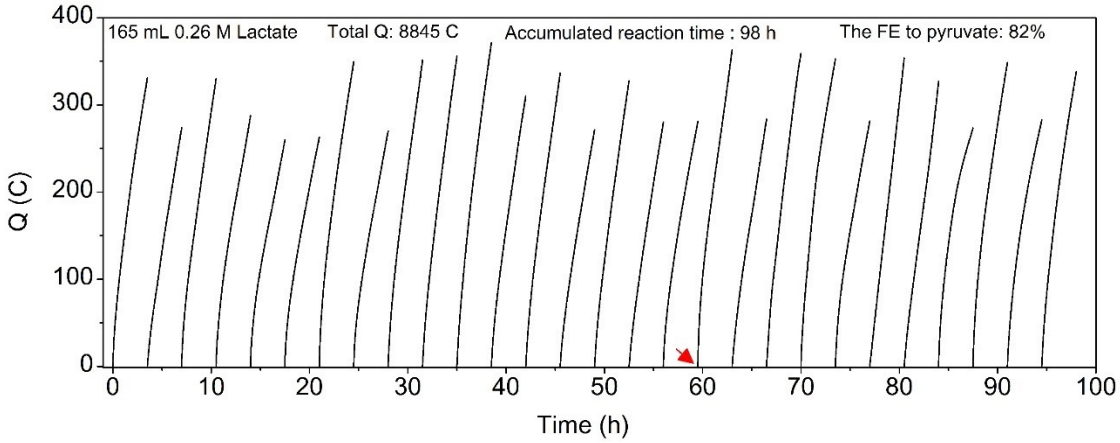

Fig. S34 Transformation of the lactate solution obtained from hydrolysis of mixed PLA plastics (4.5 g) using pulsed potential in a MEA cell at room temperature. To accelerate the lactate conversion, a larger MEA reactor equipped with the Pd/Ni(OH)$_2$/NF electrode (5 cm * 5 cm) was employed, and Pd/Ni(OH)$_2$/NF was used as both anode and cathode. To improve the pyruvate yield, closed-loop flow is used, and the flow rate is controlled to be 0.6 mL min^{-1}.

With the increase of the reaction time, the charge growth rate is decelerating, which is very common in alcohol electrooxidation.[12-13] Therefore, we deployed an intermittent strategy to implement the pulsed electrooxidation of lactate (the pulse program was reapplied every 3.5 hours). Given that the pyruvate accumulation will result in the formation of oligomer (Fig. S18), we first attempted to extract pyruvate from the anodic electrolyte after a 59.5-h pulsed electrooxidation (the pyruvate yield reaches 52.3% at this moment marked by the red arrow), and then converted the remaining lactate solution into pyruvate. We finally achieved a pyruvate yield of up to 81.5% from the PLA hydrolysate via pulsed electrooxidation.

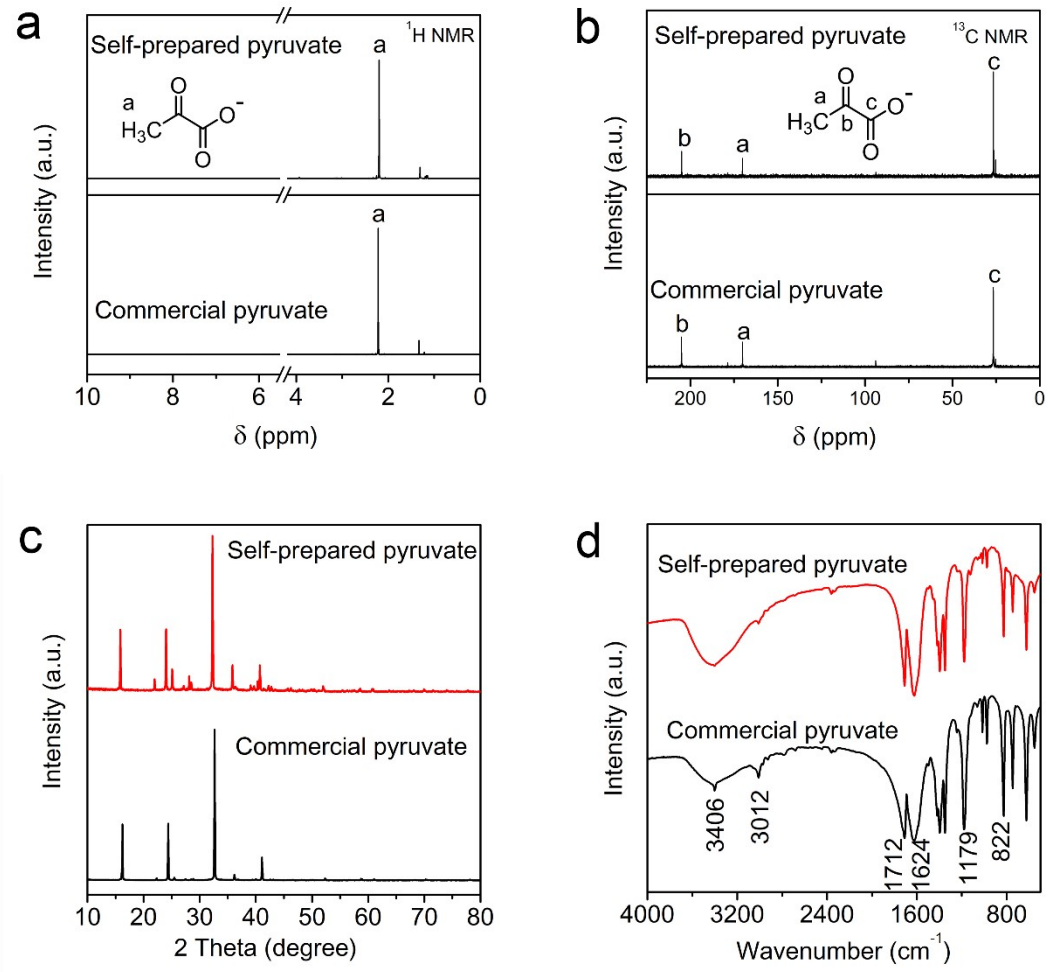

Fig. S35 (a) ^{1}H NMR spectra of pyruvate purified from the anolyte after 59.5 h of pulsed electrooxidation. (b) ^{13}C NMR spectra, (c) XRD patterns, and (d) FT-IR spectra of the self-prepared pyruvate and the commercial pyruvate.

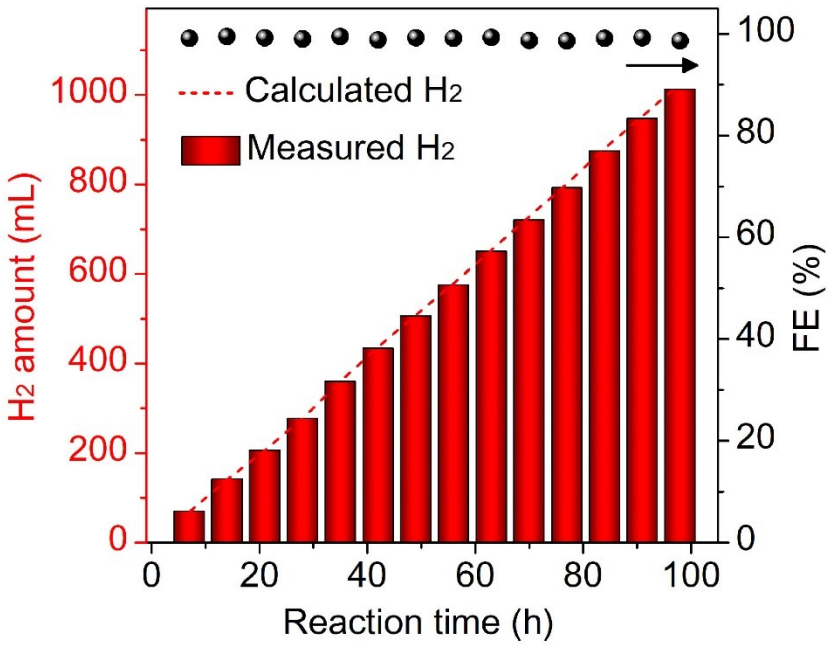

Fig. S36 H_2 amounts (1 L) collected from the cathodic H_2 evolution for 98 h.

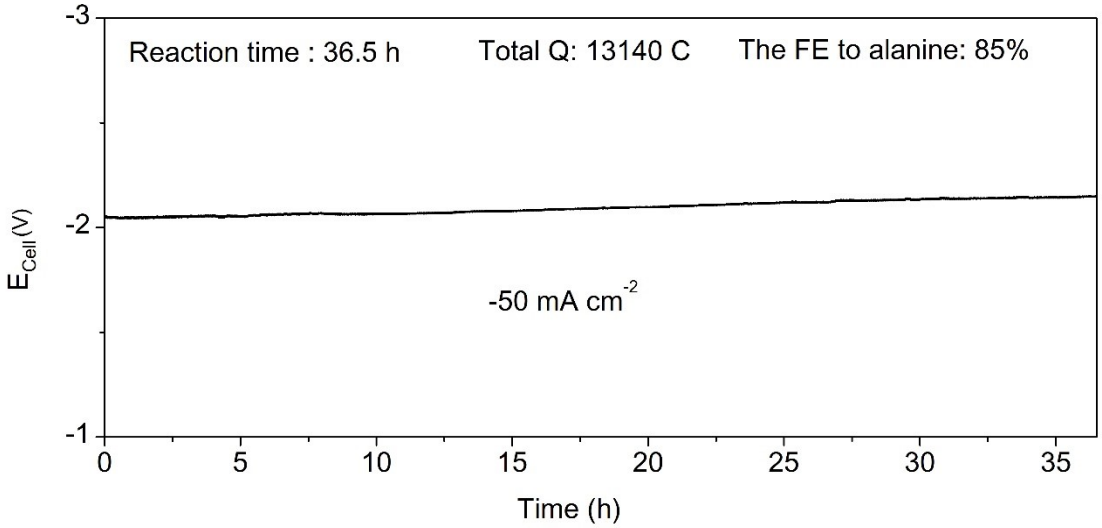

Fig. S37 Conversion of pyruvate into alanine at room temperature and the current density of -50 mA cm^{-2}. Reaction conditions: 165 mL 0.2 M H_2SO_4 catholyte containing 4.31 g potassium pyruvate (obtained from pulsed electrooxidation) and 1.13 g NH_2OH (nitrogen source), TiO_2/TF (2*2 cm, cathode), Nafion NRE-117 membrane, commercial IrO_2/TF (2*2 cm, anode), 0.5 M Na_2SO_4 (anolyte), and flow rate of 1 mL min^{-1}.

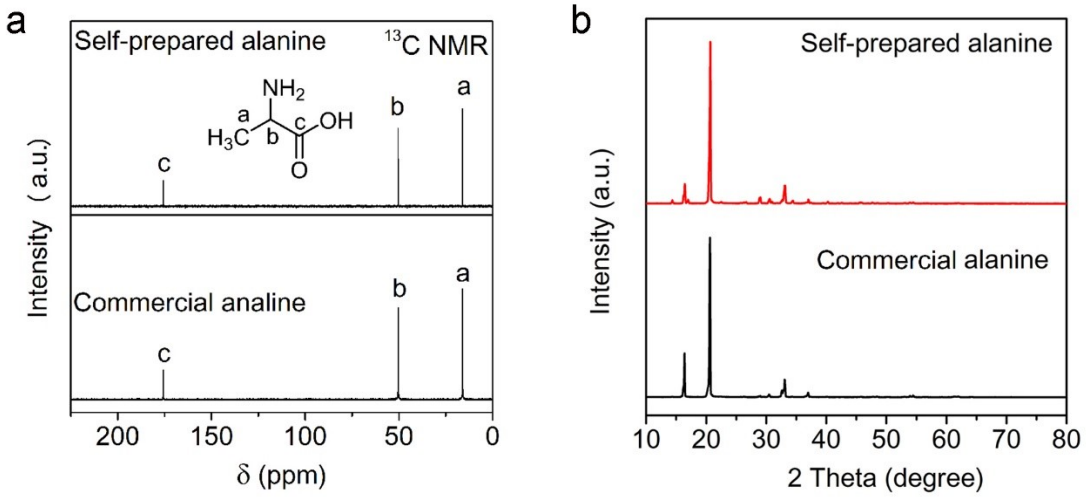

Fig. S38 (a) ^{13}C NMR spectra and (b) XRD patterns of the as-prepared alanine product and commercial alanine.

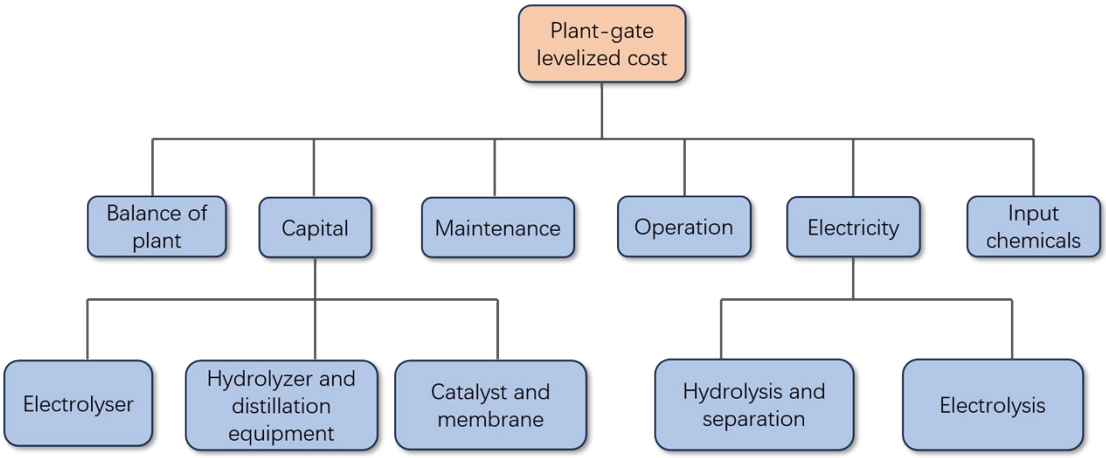

Fig. S39 The techno-economic evaluation of the plant-gate levelized PLA upcycling process.

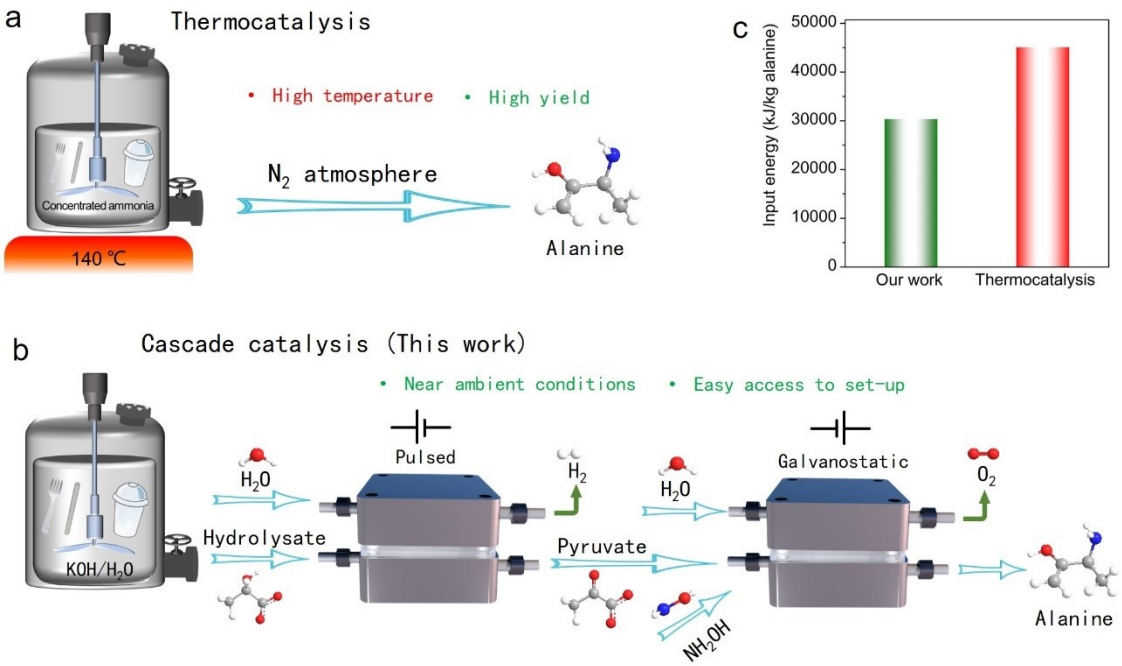

Fig. S40 Alanine production from PLA waste via thermocatalysis (a) and our cascade catalysis (b), and the thermochemical process refers to the method recently reported by Ma *et al*.[14] (c) Energy consumption comparison between thermocatalysis and our cascade catalysis.

Table S1. The comparison of j_f and j_b values of Pd/Ni(OH)$_2$/NF with different Pd loading densities, Pd/NF, and Pd/C normalized by their corresponding ECSA values. *n.a.* indicates not available.

Catalysts	Pd/Ni(OH)$_2$/NF			Pd/NF	Pd/C
Pd loading density (mg cm^{-2})	0.12	0.20	0.31	0.19	0.20
ECSA	856.5	1043.5	913.0	813.0	491.3
j_f normalized by ECSA (μA cm^{-2})	5.0	11.2	5.6	4.1	4.3
j_b normalized by ECSA (μA cm^{-2})	4.5	10.7	4.3	2.1	*n.a.*

Table S2. The price of all involved feedstocks and products.

Chemicals	Price ($/ton)	Source
Feedstocks		
Waste PLA	548	a
KOH	835	b
H_2O	0.22	[15]
H_2SO_4	45	[15]
NH_2OH	822	c
Products		
K_2SO_4	685	d
H_2	2790	[15]
O_2	82.2	e
Alanine	5206	f

a-f: Taken from the online trade market: (a) http://jiage.zz91.com/cdetail/468396.html;
(b) https://chanpin.molbase.cn/; (c) https://www.chemicalbook.com/PriceInfoall_CB8128885.htm;
(d) https://jiage.molbase.cn/hangqing/7778-80-5; (e) https://jiage.molbase.cn/hangqing/34208;
(f) https://www.100ppi.com/mprice/plist-1-9847-1.html.

Table S3. Carbon balance calculation of this integrated cascade process. 4.5 g PLA was first converted into 42.9 mmol lactate by alkali catalysis, and the remaining lactate in anodic electrolyte after pulsed electrooxidation was calculated to be 2 mmol. The consumed lactate was therefore determined to be 40.9 mmol.

Product/byproduct	Amounts (mmol)	Carbon balance
Alanine (product)	28.9	86.3%
Acetate (byproduct, evolved from pulsed electrooxidation)	3.0	
Oligomer (byproduct, evolved from pulsed electrooxidation)	Not available	
Lactate (byproduct, evolved from pyruvate reduction)	3.4	

Supplementary note 1

To evaluate the economic feasibility of this process for waste PLA upcycling, we carried out a simple techno-economic model based on our experimental results and the reported literature.[13, 16] The plant capacity for processing waste PLA is two hundred tons per day (200 tons/d). Fig. S35 summarizes the parameters used to calculate the plant-gate levelized cost of processing PLA. Table S2 provides the market value of the input chemicals and the products.
The assumptions are listed below:

1. According to the literature, we set the capital costs of the electrolyzer at $ 677 per m^2.[17-18] The total cost of the catalyst and membrane accounts for 5% of the cost of the electrolyzer.[19]
2. The electricity price is selected to be 0.05 $/kWh^{-1}.[20] The electricity costs comprise three components, electrolysis, hydrolysis, and separation. The electricity costs for the PLA hydrolysis and the products separation are assumed to be 30% of the electrolysis cost.
3. To determine the cost of equipment necessary for the depolymerization and the subsequent separation process, their combined cost is assumed to be 50% of the waste PLA feedstock cost.
4. The operation and maintenance costs are assumed to be 5% and 2.5% of the capital cost, respectively.[20]
5. The factory is anticipated to be operational on any given day with a capacity factor of 0.8, signifying that the factory will be in operation for 19.2 hours daily.[19, 21]
6. The cost of the balance of plant equipment was set as 50% of the capital cost.
7. The faradaic efficiency for pyruvate and alanine are 80% and 85%, respectively, while their corresponding faradaic efficiency for both hydrogen and oxygen are assumed to be 100%. Besides, the operation voltages for the lactate oxidation to pyruvate and oxime hydrogenation to alanine process during the two-step route are set as 0.7 V vs. RHE and 2 V under current density of 10 mA cm^{-2} and 50 mA cm^{-2} according to our experimental results.
8. The input chemicals for this process include waste PLA, potassium hydroxide, sulfuric acid, hydroxylamine hydrochloride, and water, while the output products are K_2SO4, O_2, alanine, and H_2.

The parameters required for cost calculation are determined as follows:

1. Capital costs

The electrolyzer cost. This capital cost aligns with the area of the electrolyzer. Based on the required current and the assumed operating current density, we can calculate the area of the electrolyzer needed:

$$Area\ of\ electrolyzer = \frac{I}{i}(m^2)$$

Where I is the total consumed electric current; i is the current density. The current required to sustain this process can be calculated as follows, with a capacity factor of 0.8:

$$I = \frac{Q}{Time\ in\ a\ day \times capacity\ factor}$$

Where Q is the total charge.

$$Q = \frac{Mass\ of\ ethylene\ glycol \times F \times N}{Molar\ mass\ of\ ethylene\ glycol \times Faradaic\ efficiency}$$

Where F is the Faraday's constant and N is the number of electron transfers.
Thus, the total current for the two electrolysis processes is:

$$I_1 = \frac{200 \times 10^6 \times 0.815 \times 96485 \times 2}{90 \times 0.82 \times 3600 \times 0.8} = 6166215\ A$$

$$I_2 = \frac{200 \times 10^6 \times 0.815 \times 0.874 \times 96485 \times 4}{90 \times 0.85 \times 3600 \times 0.8} = 10069444\ A$$

The electrolyzer cost can be calculated based on the estimate of $677 per m^2, therefore:

$$Cost\ of\ electrolyser = Area\ of\ electrolyser \times \$677\ per\ m^2$$

The needed electrolyzer cost was determined as follows:

$$Cost\ of\ electrolyser\ 1 = Area\ of\ electrolyser\ 1 \times 677 = 41745174\ \$$$$Cost\ of\ electrolyser\ 2 = Area\ of\ electrolyser\ 2 \times 677 = 13634028\ \$$$

The total catalyst and membrane cost are assumed to be 5 % of the electrolyzer cost and is calculated as:

$$Cost\ of\ catalyst\ and\ membrane = (Cost\ of\ electrolyser\ 1 + Cost\ of\ electrolyser\ 2) \times 5\% = 2768960\ \$$$

The capital costs of hydrolyzer and distillation equipment are assumed to be 50% of waste PLA and are calculated as:

$$The\ capital\ costs\ of\ hydrolyzer\ and\ distillation\ equipment\ =\ Cost\ of\ PLA \times 50 = 54800\ \$$$

Therefore, the capital costs per day component can be calculated as:

$$Capital\ costs = \frac{The\ electrolyzer\ cost + The\ catalyst\ and\ membrane\ costs + The\ hydrolyze}{Number\ of\ days\ in\ a\ year} = \frac{(41745174 + 13634028 + 2768960 + 54800)}{365} = 159460\ \$/d$$

2. Balance of plant

This is assumed to be 50% of the capital costs and is calculated as:

$$Balance\ of\ plant\ =\ The\ capital\ cost\ \times\ 50\% = 178833.76 \times 0.5 = 79730\ \$/d$$

3. Maintenance cost

This is assumed to be 2.5% of the capital costs and is calculated as:

$$Maintenance\ cost\ per\ day\ =\ The\ capital\ cost\ \times\ 2.5\% = 178833.76 \times 0.0025 = 3986\ \$/d$$

4. Operating cost

This is assumed to be 5% of the capital costs and is calculated as:

$$Operating\ cost\ per\ day\ =\ The\ capital\ cost\ \times\ 5\% = 178833.76 * 0.05 = 7973\ \$/d$$

5. Electricity costs：

The power required to sustain this process can be calculated as follows:

$$P\ =\ \frac{U\ \times\ I}{1000}\ (kW)$$

The energy use per day can be calculated as follows:

$$Energy\ use\ per\ day(kWh)\ =\ P\ \times\ Time\ in\ a\ day(h)\ \times\ Capacity\ factor$$

The electrolyzer electricity cost of per day can be calculated as follows:

$$Electrolyzer\ electricity\ cost\ of\ per\ day\ =\ Energy\ use\ per\ day\ \times\ Cost\ per\ kWh$$

Therefore, the electrolyzer electricity cost per day can be calculated as:

$$Electrolyzer\ electricity\ cost\ of\ per\ day\ =\ \frac{6166215\ \times\ 0.7 + 10069444 \times 2}{1000 \times 24 \times 0.8} \times 0.05 = 23477\ \$/d$$

The hydrolysis and products separation costs are assumed to be 30% of electrolyser electricity cost:

$$Hydrolysis\ and\ products\ separation\ electricity\ costs\ of\ per\ day = 23477 \times 0.3 = 7043\ \$/d$$

Therefore, the electricity cost per day can be calculated as:

$$Electricity\ costs\ per\ day = Electrolyser\ electricity\ cost\ of\ per\ day +\ Hydrolysis\ and\ products\ separ$$
$$= 23477 + 7043 = 30520\ \$/d$$

6. Input chemicals costs

For PLA hydrolysis, the input chemicals: 200 tons PLA waste, 414.81 tons KOH, and 7407.40 tons H_2O. For pyruvate separation, H_2SO_4 was utilized and the amount was equal to the mole of KOH. The mass of H_2SO_4 is 378.60 tons. Besides, pyruvate reduction to alanine requires 73.92 tons hydroxylamine hydrochloride, 109.52 tons H_2SO_4, and 5357.14 tons H_2O.

$$Input\ chemicals\ costs = mass\ of\ PLA\ waste \times cost\ of\ PLA + mass\ of\ KOH \times cost\ of\ KOH + mass\ of\ H_2SO_4 \times cost\ of\ H_2SO_4 + mass\ of\ hydroxylamine\ hydrochloride \times cost\ of\ hydroxylamine\ hydrochloride + mass\ of\ H_2O \times cost\ of\ H_2O$$
$$= 200 \times 548 + 414.81 \times 835 + (378.6 + 109.52) \times 45 + 73.92 \times 822 + (7407.4 + 5357.14) \times 0.22 = 541513.44\ \$/d$$

Finally, the total cost can be calculated by adding up all 6 components:

$$\begin{aligned} &Total\ costs \\ &= Input\ chemicals\ costs + Electricity\ costs + Capital\ costs + Maintenanc \\ &Balance\ of\ plant\ cost + Operating\ cost \\ &= 159460 + 3986 + 7973 + 79730 + 30520 + 541513.44 = 823183\ \$/d \end{aligned}$$

The products of this process include K_2SO_4, O_2, H_2, and alanine. 200 tons of PLA as raw material can obtain 645.4 tons K_2SO_4, 4.42 tons H_2, 136.68 tons alanine, and 64.92 tons O_2. Therefore, the product value can be calculated as:

$$\begin{aligned} &Product\ value \\ &= mass\ of\ alanine \times cost\ of\ alanine + mass\ of\ K_2SO_4 \times cost\ of\ K_2SO_4 + mas \\ &\times cost\ of\ H_2 + mass\ of\ O_2 \times cost\ of\ O_2 \\ &= 64.92 \times 5206 + 645.4 \times 685 + 4.42 \times 2790 + 64.92 \times 82.2 = 1171312\$/d \end{aligned}$$

Therefore, the profit can be calculated as:
$Profit = Product\ value - Total\ costs = 1171312 - 823183 = 348129\ \$/d$

Supplementary note 2

Input energy assessment

We estimate the input energy based on our experiment for PLA-to-alanine conversion and compare it with the thermal catalysis process.

The following are the assumptions made for the calculation.

1. The energy required for thermal catalytic heating can be calculated by the following formula:[22]
   $Q = C_P \times m \times \Delta T$
   Where m represents the mass reactant in the reactor, C_p is the heat capacity (set as 4.2 kJ/kg℃), and ΔT is the temperature difference.
2. The power required to sustain this process can be calculated as follows:
   $$P = \frac{U \times I}{1000}\ (kW)$$
   The electric energy use can be calculated as follows:
   $Electric\ energy\ use\ (kJ) = P \times Time\ (h) \times 3600$
   One kilowatt-hour (kWh) is equal to 3600 kJ.

Cascade catalysis (This work)

1. PLA hydrolysis
   To hydrolyze 4.5 g of PLA, 165 mL of water and 12 g of potassium hydroxide are needed and heated to 60°C. The thermal energy required for this process is as follows:
   $Thermal\ energy = C_P \times m \times \Delta T = 24.84kJ$
2. Based on our experiment, it takes 98 hours to produce pyruvic acid from lactic acid by electrochemical oxidation, with a current of 0.1 A and a voltage of 0.7 V in the electrolytic cell. Besides, it takes 36.5 hours to reduce pyruvic acid to alanine by electrochemical reduction, with a voltage of 2 V and a current of 0.1 A in the electrolytic cell. The electric energy required for this process is as follows:
   $Electric\ energy\ (kJ) = P \times Time\ (h) \times 3600 = 50.98kJ$
3. This process produced 2.5 g of alanine. Therefore, the energy input required for the production of one kilogram of alanine is:
   $$Iput\ energy\ (kJ/kg\ alanine) = \frac{(24.84 + 50.98)}{2.5} \times 1000 = 30328kJ/kg\ alanine$$

Thermochemical process

We also calculated the input energy for the thermochemical process based on the literature.[14] To convert 5 g of PLA to alanine, 30 mL of ammonia is needed and heated to 140°C, and the cycle is repeated eight times. The electric energy required for this process is as follows:

$$Thermal\ energy = C_P \times m \times \Delta T \times 8 = 135.24kJ$$

This process produced 3 g of alanine. Therefore, the energy input required for production of one kilogram of alanine is:

$$Iput\ energy\ (kJ/kg\ alanine) = \frac{135.24}{3} \times 1000 = 45080kJ/kg\ alanine$$

References

[1] Y. Zheng, Y. Jiao, Y. Zhu, L. H. Li, Y. Han, Y. Chen, M. Jaroniec, S.-Z. Qiao, *J. Am. Chem. Soc.* **2016**, *138*, 16174-16181.

[2] Z. Li, Y. Yan, S.-M. Xu, H. Zhou, M. Xu, L. Ma, M. Shao, X. Kong, B. Wang, L. Zheng, *Nat. Commun.* **2022**, *13*, 147.

[3] V. Tournier, C. Topham, A. Gilles, B. David, C. Folgoas, E. Moya-Leclair, E. Kamionka, M.-L. Desrousseaux, H. Texier, S. Gavalda, *Nature* **2020**, *580*, 216-219.

[4] X. Liu, M. Gong, S. Deng, T. Zhao, T. Shen, J. Zhang, D. Wang, *Adv. Funct. Mater.* **2021**, *31*, 2009032.

[5] L. Deng, F. Hu, M. Ma, S. C. Huang, Y. Xiong, H. Y. Chen, L. Li, S. Peng, *Angew. Chem. Int. Ed.* **2021**, *60*, 22276-22282.

[6] D. Y. Chung, K.-J. Lee, Y.-E. Sung, *J. Phys. Chem. C.* **2016**, *120*, 9028-9035.

[7] A. C. Rios, P. P. Bera, J. A. Moreno, G. Cooper, *ACS Omega* **2020**, *5*, 15063-15068.

[8] D. Martín‐Yerga, J. White, G. Henriksson, A. Cornell, *ChemSusChem* **2021**, *14*, 1902-1912.

[9] N. Wu, J. Wang, D. N. Tafen, H. Wang, J.-G. Zheng, J. P. Lewis, X. Liu, S. S. Leonard, A. Manivannan, *J. Am. Chem. Soc.* **2010**, *132*, 6679-6685.

[10] T. Fukushima, M. Yamauchi, *Chem. Commun.* **2019**, *55*, 14721-14724.

[11] Y. Xu, Z. Li, L. Gao, D. Zhang, X. Zhao, S. Wang, Y. Wang, *Ind. Eng. Chem. Res.* **2015**, *54*, 1068-1073.

[12] Y. Yan, H. Zhou, S.-M. Xu, J. Yang, P. Hao, X. Cai, Y. Ren, M. Xu, X. Kong, M. Shao, *J. Am. Chem. Soc.* **2023**, *145*, 6144-6155.

[13] H. Zhou, Y. Ren, Z. Li, M. Xu, Y. Wang, R. Ge, X. Kong, L. Zheng, H. Duan, *Nat. Commun.* **2021**, *12*, 4679.

[14] S. Tian, Y. Jiao, Z. Gao, Y. Xu, L. Fu, H. Fu, W. Zhou, C. Hu, G. Liu, M. Wang, D. Ma, *J. Am. Chem. Soc.* **2021**, *143*, 16358-16363.

[15] W.-J. Liu, Z. Xu, D. Zhao, X.-Q. Pan, H.-C. Li, X. Hu, Z.-Y. Fan, W.-K. Wang, G.-H. Zhao, S. Jin, G. W. Huber, H.-Q. Yu, *Nat. Commun.* **2020**, *11*, 265.

[16] Y. Lum, J. E. Huang, Z. Wang, M. Luo, D.-H. Nam, W. R. Leow, B. Chen, J. Wicks, Y. C. Li, Y. Wang, C.-T. Dinh, J. Li, T.-T. Zhuang, F. Li, T.-K. Sham, D. Sinton, E. H. Sargent, *Nat. Catal.* **2020**, *3*, 14-22.

[17] M. Li, Y. Wu, B.-H. Zhao, C. Cheng, J. Zhao, C. Liu, B. Zhang, *Nat. Catal.* **2023**, 6, 906–915.

[18] A. T. Mayyas, M. F. Ruth, B. S. Pivovar, G. Bender, K. B. Wipke, National Renewable Energy Lab.(NREL), Golden, CO (United States), **2019**.
[19] W. R. Leow, Y. Lum, A. Ozden, Y. Wang, D.-H. Nam, B. Chen, J. Wicks, T.-T. Zhuang, F. Li, D. Sinton, E. H. Sargent, *Science* **2020**, *368*, 1228-1233.
[20] H. Shin, K. U. Hansen, F. Jiao, *Nature Sustainability* **2021**, *4*, 911-919.
[21] P. De Luna, C. Hahn, D. Higgins, S. A. Jaffer, T. F. Jaramillo, E. H. Sargent, *Science* **2019**, *364*, eaav3506.
[22] S. Abrahms-Kavunenko, *J. Mater. Cult.* **2023**, *28*, 3-23.